Supplementary Methods and Results, Figures and Tables

Genome-wide analysis of chromatin states reveals distinct mechanisms of sex-dependent gene regulation in male and female mouse liver, Molec Cell Biol (2013).

Aarathi Sugathan and David J. Waxman, Boston University

All Supplementary text, figures and tables listed here are included in this pdf, except for tables in Excel format, which can be found in Supplemental Files 2-10, as noted below).

Supplementary Methods and Results *(p. 2-7)*

Supplementary Figures *(p. 8-42)*

List of Supplementary Tables *(p. 43-61)*

Supplementary Methods and Results

1. Analysis of Data Quality (Table S7, p. 54-61)

For each chromatin modification in each sex, biological replicates were evaluated for data quality using four metrics: **1)** Percentage of mapped reads that fall in 'straight peaks', defined as 5 or more identical reads (i.e., that map to the same genomic position) and do not overlap any other mapped reads; **2)** Frequency of overlap between peaks/regions identified separately in each individual replicate using MACS (Zhang et al. 2008) or SICER (Zang et al. 2009); **3)** After merging peaks/regions identified in all individual replicates, the correlation between the number of reads in peaks from each replicate was calculated; **4)** To confirm results for K4me1 and K4me3, the peak overlap with DHS (Ling et al. 2010) and with K4me1/me3 peaks from another lab (Robertson et al. 2008) were compared. These comparisons are shown in Table S7.

Using these metrics, two K27me3 samples (one male and one female liver sample) were excluded due to reads in straight peaks making up >4% of total mapped reads, compared to <1% for all other samples. These two samples also had much lower peak overlap with the other K27me3 replicates. Further, although the K9me3 biological replicates displayed low peak overlap (~30%), no samples were excluded, as the correlations between reads in peaks were >0.8, and each replicate had < 1% of reads in straight peaks. K36me3 and K27ac had very high peak overlap and very high read count correlations – for K36me3, the lowest correlation was 0.96 and the lowest peak overlap 87%; for K27ac the lowest correlation was 0.96 and the lowest peak overlap 78%. Therefore no replicates were excluded for K9me3, K36me3, and K27ac.

One K4me1 male liver sample consistently showed low peak overlap with the other male K4me1 replicates (as low as 24%), which was consistent with a lower read count correlation between this and other samples (as low as 0.54). In contrast, the other K4me1 male samples had a minimum peak overlap of 69% and minimum correlation of 0.70. One K4me3 sample, which was obtained from the same mouse, was similarly an outlier compared to the other K4me3 male samples, but not to the same extent (minimum peak overlap 70% and minimum correlation 0.91). To confirm that these two samples are inconsistent with the other replicates, we compared peaks from each K4me1 and K4me3 replicate with DHS peaks at two levels of stringency (Ling et al., 2010) and with K4me1 and K4me3 peaks identified in female mouse liver by Robertson et al (2008). These comparisons showed that the two samples with low concordance with other replicates also have significantly lower overlap with DHS and with Robertson's peaks compared to other K4me1 and K4me3 replicates. Therefore, these two samples were excluded from further analysis.

2. Chromatin States in Mouse Liver (Fig. 2; Fig. S3, p. 13-14)

The six chromatin mark datasets along with DNase hypersensitivity (Ling et al., 2010) were analyzed together for chromatin states using ChromHMM (Ernst et al., 2011), to learn a hidden Markov model to assign chromatin states across the mouse genome. ChromHMM was run using an IgG control and with default parameters. A single joint model was learned for male liver and female liver. Ernst et al (2011) found a 15-state model to be informative for the human genome.

We therefore started with 20 states and used the ChromHMM CompareModels module to compare decreasing numbers of states to the 20-state model. For each of the 20 states, we calculated similarity – i.e. the correlation between emission parameters – to its closest state in models with smaller numbers of states (Fig. S3B). By decreasing the number of states in the model, individual states in the 20-state model are progressively lost. Going from a 20-state model down to a 15-state model, zero or one additional state is lost at each step with < 0.9 correlation (Fig. S3C). No additional states were lost (< 0.9 correlation) when going from a 15-state to a 14-state model, whereas when going from a 14-state to a 13-state model, two additional states have correlation < 0.9 and < 0.8, with further increasing dissimilarity after 12 states (Fig. S3C). Therefore, a 14-state model was chosen for mouse liver based on our data.

3. Classification of sex-biased genes (Fig. 4; Fig. S6, p. 19-23; Table S4A, p. 46)

Genes that show sex-biased expression (423 male-biased genes and 477 female-biased genes) were clustered by their chromatin mark and DHS densities around the TSS and TES in male liver, and separately, in female liver (Fig. S6A). Three gene clusters that differ in chromatin state and, correspondingly, in the level of gene expression, were thus obtained for each sex (Fig. S6B-C): active (high levels of activating marks around both the TSS and TES), intermediate (high levels of activating marks around the TSS only), and inactive chromatin state (low levels of activating marks, high level of K27me3). The active and intermediate sex-biased gene clusters were primarily comprised of genes in the active clusters among all genes (cluster 1 and clusters 2 and 3 of Fig. 3, respectively), while the inactive sex-biased gene clusters correspond to the poised and inactive clusters among all genes (clusters 4-6 of Fig. 3) (Fig. S6D). The sex-biased genes were then grouped into 6 female-biased and 6 male-biased gene classes, F1-F6 and M1-M6 respectively, based on their chromatin activity classification in each sex (Table S4A). Next, the genes in each class were characterized with regard to the sex-specificity of their chromatin environments. To do this, we first compared normalized densities of each of the six marks on a genome-wide basis in male vs. female liver and thereby identified genomic regions that showed significant male enrichment or female enrichment for each chromatin mark (Table S3). The distribution of sex-biased and sex-independent chromatin marks was then determined for the genes in each class (Fig. S6E, listed in Table S1, B-C).

A majority of sex-biased genes belonged to the same chromatin-based cluster in both male and female liver (classes F1, F2, and M1, M2 in Table S4), and were primarily associated with sex-independent chromatin marks (Fig. 4A and Fig. S6E), with a high fraction of F1 and M1 genes containing activating marks and a high fraction of F2 and M2 genes containing K27me3 or lacking activating marks, consistent with the chromatin activity status designations shown in Table S4A. Other sex-biased genes (classes F3, F4 and M3, M4) belong to a more active chromatin cluster in the sex where the gene is more highly expressed, and correspondingly, classes F3, M3 and M4 (but not F4) displayed sex-enriched chromatin marks at comparatively high frequencies (Fig. 4A). Class F3 and M3 genes also showed the largest sex-differences in expression (Fig. 4B). Thus, classes F3, M3, and M4 represent genes that have sex-biased chromatin marks in their immediate vicinity. However, these classes represent only 5.6% of all sex-biased genes, consistent with the

conclusion that many sex-biased genes are not in a sex-biased chromatin environment (c.f. Fig. 2F). Indeed, taking into account distal chromatin marks, which may represent distal regulatory sites, less than half of sex-biased genes have sex-biased chromatin marks within 10 kb, and only 66-69% within 100 kb (Fig. S6F). Genes that belong to the inactive chromatin cluster in the sex in which they were more highly expressed (classes F2, F5, M2, M5) are more likely than others to have a sex-independent K27me3 domain (Fig. S6E).

4. Characteristics of sex-biased genes ranked by expression sex ratio (Fig. S7, p. 24-25)

Female-biased genes, and separately male-biased genes, were divided into four subgroups according to the magnitude of sex-difference in gene expression. Genes in each of the four groups were examined for the occurrence of sex-biased local chromatin marks (Fig. S7A) and for enrichment for being targets for each of the TFs of interest (Fig. S7B). Since each subgroup contains the same number of genes (118-121 genes in each group for female-biased genes, and 103-108 genes in each group for male-biased genes), the number of genes in each group does not affect the analysis. Our findings support the following conclusions made from Fig. 4 and Fig. 5: Male-enriched K27me3 marks the most highly female-biased genes (Fig. S7A, top panel), while male-biased genes lack female-enriched K27me3 (Fig. S7A, bottom panel). Among female-biased genes, those that are most highly female-biased in expression frequently exhibit sex-differences in proximal chromatin marks (Fig. S7A, top panel). Gene class F3 contains the most highly female-biased genes (Fig. 4B); F3 genes (Fig. 5A), as well as the top quarter of female-biased genes by gene expression sex ratio (Fig. S7B), are enriched for being gene targets of STAT5 and FOXA2, while BCL6 targets are enriched among genes that lack sex-differences in proximal chromatin marks (Fig. 5A) and genes that are weakly female-biased in expression (Fig. S7B).

5. Preference of categories of DHS sites to be mapped to categories of sex-biased genes (Table S5B-D, p. 18)

Each DHS was mapped to its nearest gene TSS within 250 kb; specifically, the nearest sex-biased gene TSS for sex-biased DHS, and nearest liver-expressed gene TSS for sex-independent DHS. The preference for each type of male-biased DHS site, D_i (summarized in Table S5A) to be mapped to each class of sex-biased gene G_j (listed in Table S4A) was computed as an enrichment (Table S5B):

$$\frac{(\text{\# male-biased DHS sites of type } D_i \text{ with nearest TSS in class } G_j)/(\text{\# total male-biased DHS of type } D_i)}{\sum_i (\text{DHS sites of type } D_i \text{ with nearest TSS in class } G_j)/(\text{\# total male-biased DHS sites})}$$

A similar calculation was performed for categories of female-biased DHS sites and of sex-independent DHS sites. For sex-independent DHS sites, only those whose nearest gene was sex-biased were included in the background.

Tables S5B and S5C show that sex-biased gene classes F3 and M3, which comprise the most highly sex-biased genes, are enriched for association (within 250 kb) with sex-biased DHS that have sex-biased K27ac, the mark of an active enhancer. Similarly, among sex-independent DHS

(Table S5D), the highest enrichments are for association between sites with sex-biased K27ac and F3 and M3 genes. For class F3 but not class M3 genes, the enrichment is independent of K4me1 status. Some male-biased DHS also show enrichment for association with female-biased genes (Table S5C); these may be repressive regulatory sites.

6. Correlation of TF binding with DHS/chromatin mark sex ratios (Fig. S8, Fig. S9, p. 26-28)

Figure S8 A-H: The set of 72,862 merged DHS (Ling et al., 2010) was ranked by male-female ratio after normalization by reads in male-female liver common peaks. The DHS were ranked separately by male-female ratio in DNase hypersensitivity, and by K4me1, K27ac, and K27me3 read density over the entire peak region, and the ranked DHS then divided into bins of 1,000 DHS each. For each TF, the fraction of TF binding sites that overlapped a DHS in each bin was determined. A TF binding sites was considered to overlap a DHS if the ChIP-Seq peak region identified for the TF overlapped the DHS peak region by at least one base pair.

Figure S9 A-E: The following approach was used to determine if there is a relationship between the either sex ratio or intensity of TF binding and the sex ratio DNase hypersensitivity or chromatin modifications. For TF binding sites that overlap DHS, the sex ratio in TF binding (STAT5, FOXA1, and FOXA2) or TF binding intensity (BCL6 and CUX2) was plotted against the sex ratio in DNase hypersensitivity, or in K4me1, K27ac, and K27me3 marks. Pearson's correlation was then calculated for each plot. For BCL6 and CUX2, robust linear regression of TF binding intensity (ChIP-seq read density) against sex ratio in DHS/K4me1/K27ac/K27me3 is shown in green.

7. Characterization of DHS by enhancer modifications, target gene class, and enrichment of TF binding (Table S6, p. 53 and Excel file; related to Fig. 6)

The categorization of DHS by enhancer modifications is depicted in Table S6A.

Tables S6 B-D show enrichments for TF binding at categories of male-biased (B), female-biased (C), and sex-independent (D) DHS, shown in Fig. 6B, and also for subsets of each category of DHS that map to different classes of sex-biased genes.

To obtain target genes, each DHS was mapped to the nearest gene TSS within 250 kb; specifically, the nearest TSS of a sex-biased gene for sex-biased DHS, and to the nearest liver-expressed gene TSS for sex-independent DHS. The 250 kb limit was chosen based on the observation made using 5C technology (Sanyal et al., 2012) that most long-range interactions occur within 250 kb of the TSS, and the frequency of interactions peaks ~120 kb upstream of the TSS. Enrichments for TF binding were calculated for each category of sex-biased DHS, and for sex-independent DHS whose nearest gene TSS was sex-biased in its expression. Tables S6 B-D also show the numbers of DHS in each enriched or depleted group and their associated p-value.

8. Sex-difference in K4me1 profile (Fig. S10D-S10H, p. 30-34; related to Fig. 7)

Figures S10 D-E: *Quantification of K4me1 distribution and sex-difference.*

For each type of DHS in each sex, to calculate the depth of the K4me1 trough, the K4me1 read density at the DHS summit is subtracted from the K4me1 read density at the K4me1 maximum (i.e., the position at which K4me1 forms a local maximum where there are bimodal peaks). Where K4me1 forms a trough, this value is positive, and if K4me1 forms a single monomodal peak, this value is negative. The sex-difference in K4me1 distribution was computed as the difference between this value in male and female liver:

$$[(\text{K4me1 max} - \text{DHS summit})_{\text{male}} - (\text{K4me1 max} - \text{DHS summit})_{\text{female}}].$$

These values are shown in Fig. S10D.

For each set of TF binding sites (FOXA1-male, FOXA2-male, STAT5-male, and CUX2) at male-biased DHS sites, the difference in K4me1 profile between male and female liver is compared with and without binding of a second factor. These are shown in Fig. S10E. For STAT5, the K4me1 profile difference is greatly intensified when STAT5 binds along with FOXA1/2 or CUX2.

Figs. S10 F-H: *K4me1 profile at non-FOXA binding male-biased DHS sites sampled to match FOXA-binding sites in DHS intensity or DHS sex ratio.*

A Wilcoxon signed rank test was used to compare the DHS sex ratio and DHS read intensity in male liver between male-biased DHS that bind FOXA1/FOXA2 in a male-enriched or sex-independent manner to those that do not bind FOXA1/FOXA2. Fig. S10F shows p-values for FOXA1 and FOXA2 in the first table. These results show that DHS where FOXA1/FOXA2 bind are more intense than those where the FOXA factors do not bind, and DHS where FOXA1/FOXA2 bind in a male-enriched manner are more sex-biased than those where they do not bind. This is what we would expect if FOXA1 and FOXA2 have chromatin opening activity.

In order to determine whether the deep trough in the K4me1 profile in male liver is related to FOXA1/FOXA2 binding, rather than just a feature of highly DNase hypersensitive sites or DHS with high male/female ratio in hypersensitivity regardless of FOXA1/FOXA2 binding, samples were chosen from the non-FOXA binding set that matched the distributions in DHS intensity or DHS male/female ratio exhibited by the FOXA binding sets. For each FOXA1/FOXA2 binding set, a matched non-FOXA binding set was chosen from male-biased DHS that bind neither FOXA1 nor FOXA2, either sex-independently or in a male-enriched manner. P-values of significance for difference between each FOXA binding set and its matched non-FOXA binding set are shown in the second table of Fig. S10F.

Figs. S10G and S10H show K4me1 profiles at FOXA1-male-enriched binding sites, FOXA1-sex-independent binding sites, FOXA2-male-enriched binding sites, and FOXA2-sex-independent binding sites, each compared to a matched background set of non-FOXA binding sites. The background sets were matched by either DHS intensity in male (Fig. S10G) or DHS sex ratio (Fig. S10H). These figures support the conclusions from Fig. 7: (1) sites with male-enriched FOXA1/FOXA2 have a deeper trough in K4me1 marks in male liver compared to those that lack

FOXA binding, and (2) sites with sex-independent FOXA1/FOXA2 binding have a bimodal K4me1 peak in both male liver and female liver, while those that lack FOXA binding have a monomodal K4me1 peak in female liver.

Supplementary References

Ernst J, Kheradpour P, Mikkelsen TS, Shoresh N, Ward LD, Epstein CB, Zhang X, Wang L, Issner R, Coyne M et al: **Mapping and analysis of chromatin state dynamics in nine human cell types.** Nature 2011, 473(7345):43-49.

Ling G, Sugathan A, Mazor T, Fraenkel E, Waxman DJ: **Unbiased, genome-wide in vivo mapping of transcriptional regulatory elements reveals sex differences in chromatin structure associated with sex-specific liver gene expression**. *Mol Cell Biol* 2010, **30**(23):5531-5544.

Robertson AG, Bilenky M, Tam A, Zhao Y, Zeng T, Thiessen N, Cezard T, Fejes AP, Wederell ED, Cullum R *et al*: **Genome-wide relationship between histone H3 lysine 4 mono- and tri-methylation and transcription factor binding.** *Genome Res* 2008, **18**(12):1906-1917.

Shin H, Liu T, Manrai AK, Liu XS: **CEAS: cis-regulatory element annotation system.** *Bioinformatics* 2009, **25**(19):2605-2606.

Zang C, Schones DE, Zeng C, Cui K, Zhao K, Peng W: **A clustering approach for identification of enriched domains from histone modification ChIP-Seq data**. *Bioinformatics* 2009, **25**(15):1952-1958.

Zhang Y, Liu T, Meyer CA, Eeckhoute J, Johnson DS, Bernstein BE, Nusbaum C, Myers RM, Brown M, Li W *et al*: **Model-based analysis of ChIP-Seq (MACS)**. *Genome Biol* 2008, **9**(9):R137.

Supp Fig. S1A: correlations between chromatin modifications and gene expression as measured by RNA-seq or by Microarray (Wauthier et al., 2010).

All genes, male liver

	K9me3_coding	K27me3_coding	K4me1_coding	K27ac_coding	K27ac_promoter	K4me3_promoter	K36me3_coding	**RNAseq**	Microarray
K9me3_coding		0.54	-0.31	-0.38	-0.42	-0.37	-0.39	-0.41	-0.33
K27me3_coding	0.54		-0.56	-0.69	-0.73	-0.66	-0.73	-0.73	-0.61
K4me1_coding	-0.31	-0.56		0.87	0.69	0.60	0.58	0.65	0.58
K27ac_coding	-0.38	-0.69	0.87		0.77	0.63	0.66	0.72	0.65
K27ac_promoter	-0.42	-0.73	0.69	0.77		0.89	0.78	0.79	0.67
K4me3_promoter	-0.37	-0.66	0.60	0.63	0.89		0.73	0.73	0.60
K36me3_coding	-0.39	-0.73	0.58	0.66	0.78	0.73		0.79	0.64
RNAseq	-0.41	-0.73	0.65	0.72	0.79	0.73	0.79		0.79
Microarray	-0.33	-0.61	0.58	0.65	0.67	0.60	0.64	0.79	

Liver-expressed genes, male liver

	K9me3_coding	K27me3_coding	K4me1_coding	K27ac_coding	K27ac_promoter	K4me3_promoter	K36me3_coding	**RNAseq**	Microarray
K9me3_coding		0.43	-0.18	-0.20	-0.23	-0.16	-0.19	-0.23	-0.16
K27me3_coding	0.43		-0.48	-0.53	-0.53	-0.42	-0.47	-0.43	-0.30
K4me1_coding	-0.18	-0.48		0.85	0.45	0.31	0.17	0.42	0.33
K27ac_coding	-0.20	-0.53	0.85		0.47	0.30	0.18	0.47	0.40
K27ac_promoter	-0.23	-0.53	0.45	0.47		0.86	0.46	0.35	0.25
K4me3_promoter	-0.16	-0.42	0.31	0.30	0.86		0.44	0.24	0.16
K36me3_coding	-0.19	-0.47	0.17	0.18	0.46	0.44		0.43	0.22
RNAseq	-0.23	-0.43	0.42	0.47	0.35	0.24	0.43		0.53
Microarray	-0.16	-0.30	0.33	0.40	0.25	0.16	0.22	0.53	

Supp Fig. S1B – M/F ratio in numbers of reads for each chromosome

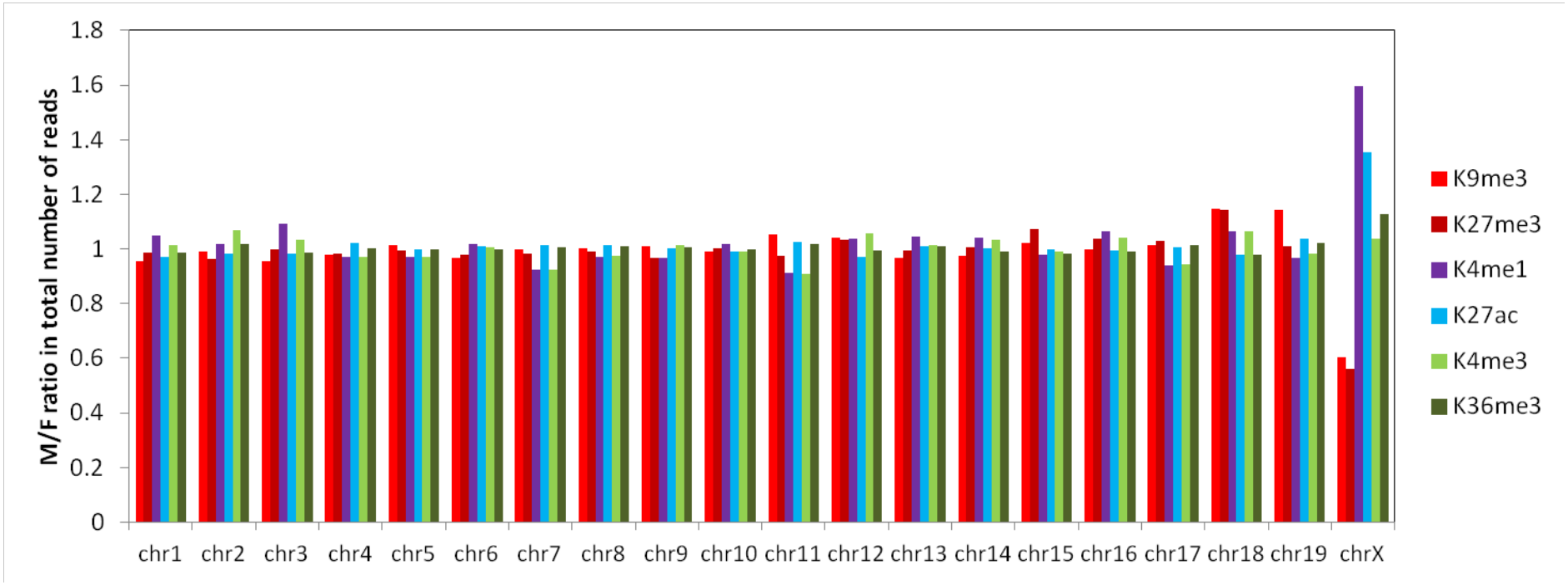

Supp Fig. S2A Genomic localization of reads for each of the six chromatin modifications, generated using CEAS (Shin et al., 2009). K9me3 is mostly intergenic: 67% of K9me3 reads are intergenic, compared to 50% for K27me3 and ≤ 25% for each of the other marks.

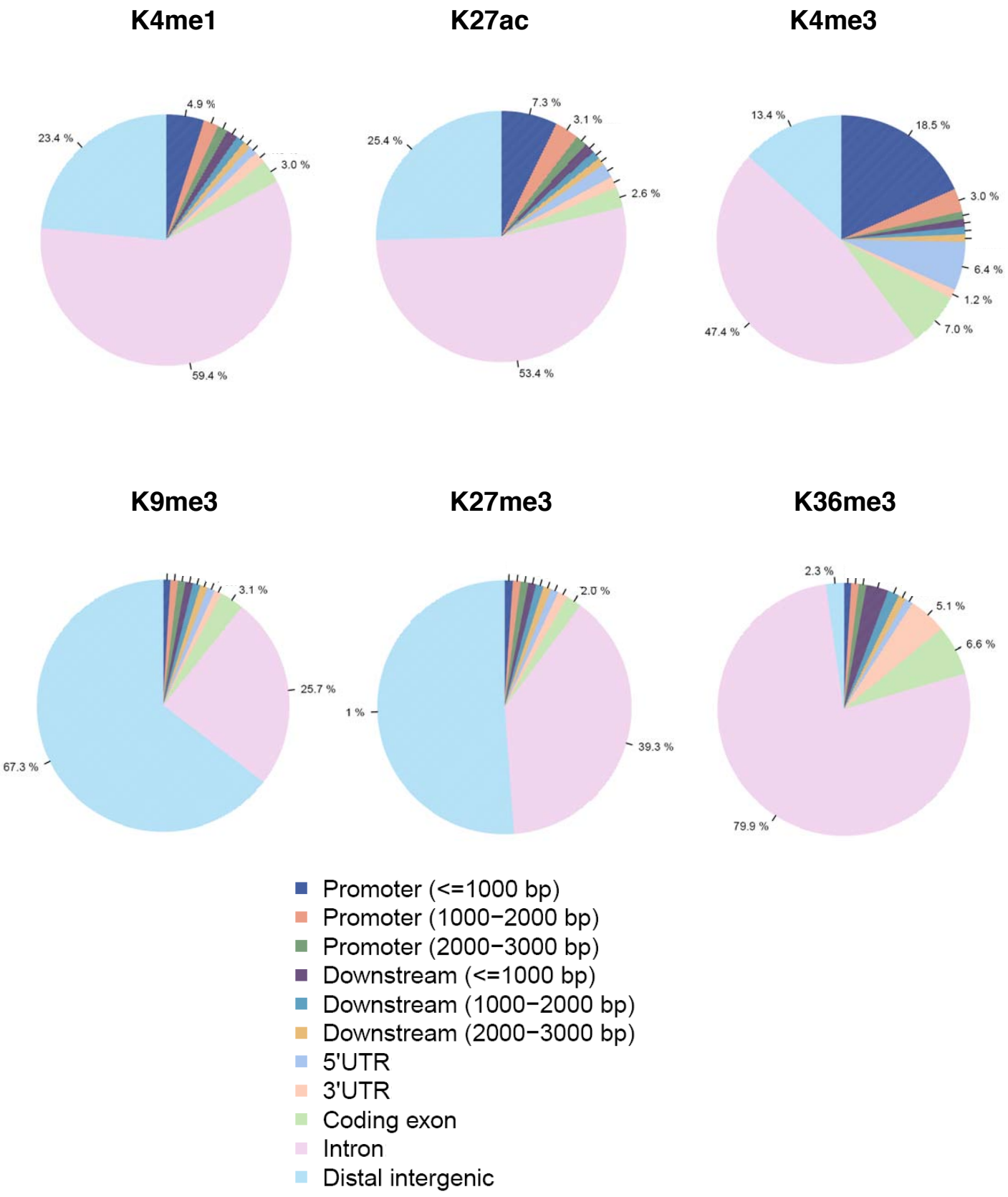

Supp Fig. S2B Read profiles across gene bodies and at TSSs for each mark at three sets of genes: top 1000 by expression in liver, middle 1000 by expression in liver, and bottom 1000 by expression in liver. Figures were generated using CEAS (Shin et al., 2009).

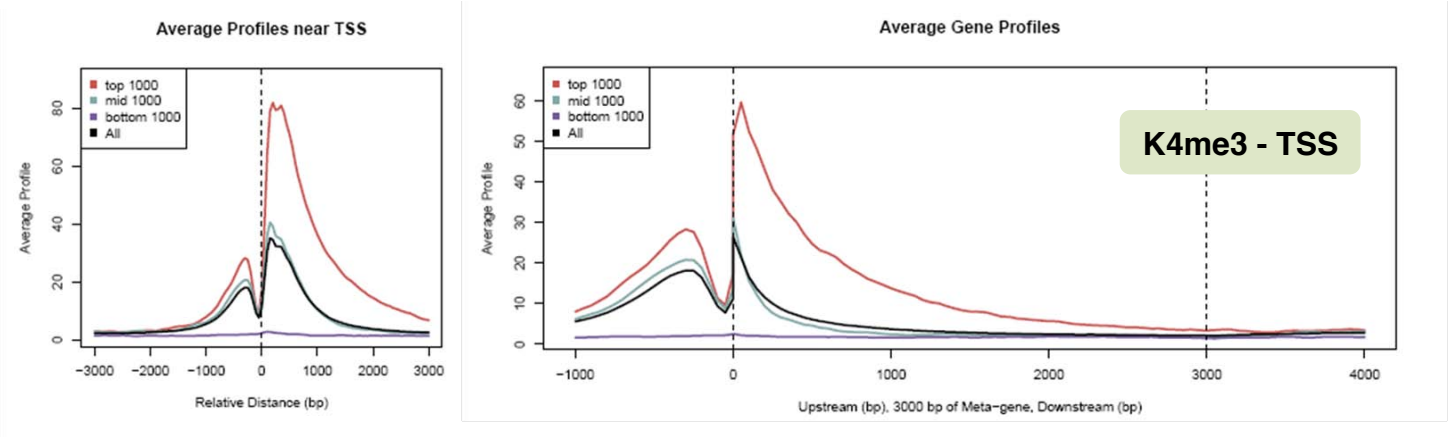

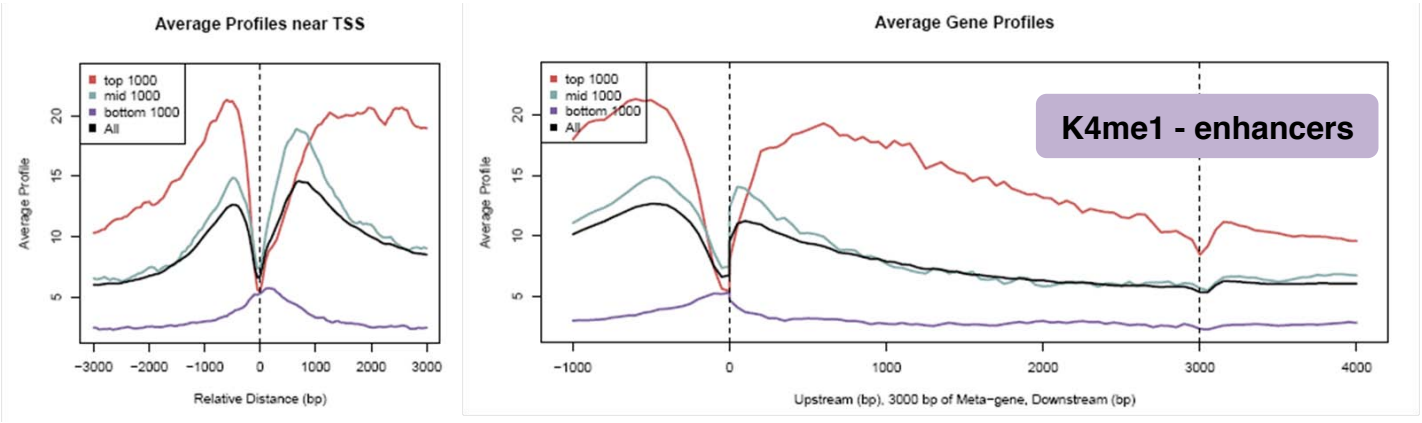

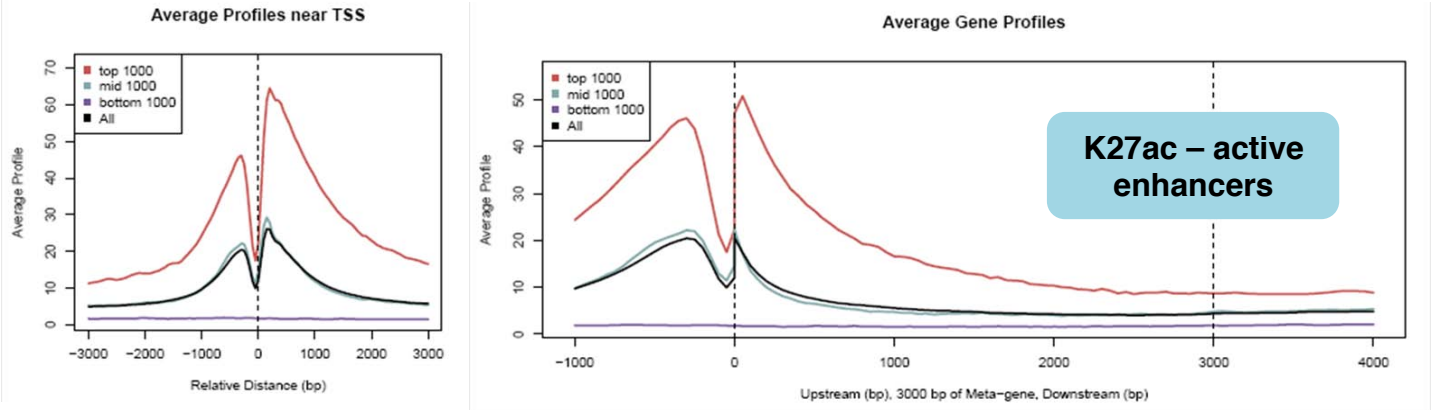

Supp Fig. S2B continued Read profiles across gene bodies for each mark at three sets of genes: top 1000 by expression in liver, middle 1000 by expression in liver, and bottom 1000 by expression in liver. Figures were generated using CEAS (Shin et al., 2009).

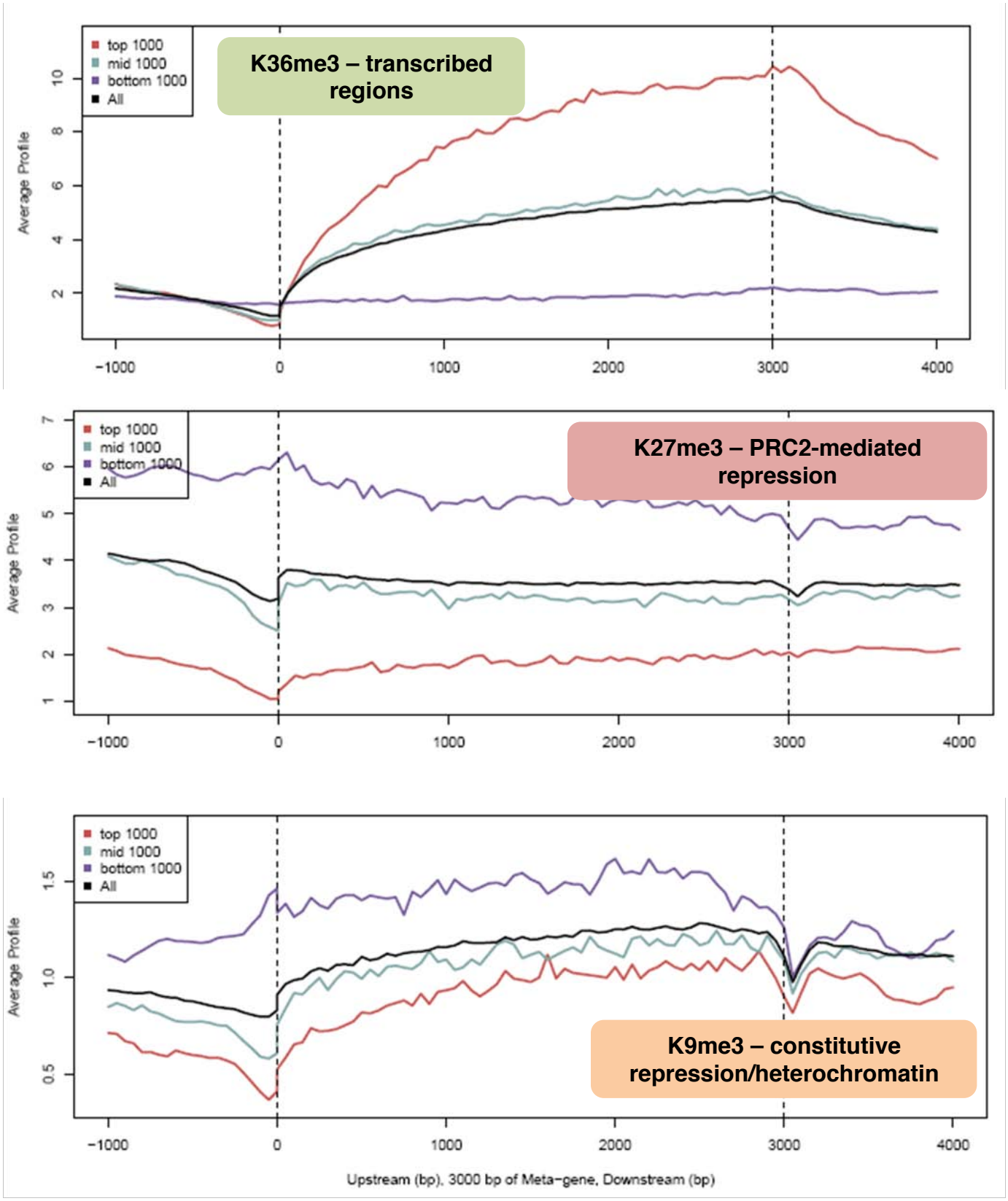

Supp Fig. S3A – Emission and Transition parameters for 14 chromatin states in mouse liver determined by ChromHMM.

- Repressive states
  - **State1** (K27me3)
  - **State3** (K9me3)
  - **State2** (?)
- Active states
  - **States 7 and 8**: promoter (K4me3)
  - **State14**: transcribed (K36me3)
  - **State13**: transcribed (?)
  - **States 5-6, 9-11**: enhancers with different combinations of K27ac, K4me1, DHS.
- Other
  - **State12**: K27me3 with activating marks
  - **State4**: no marks

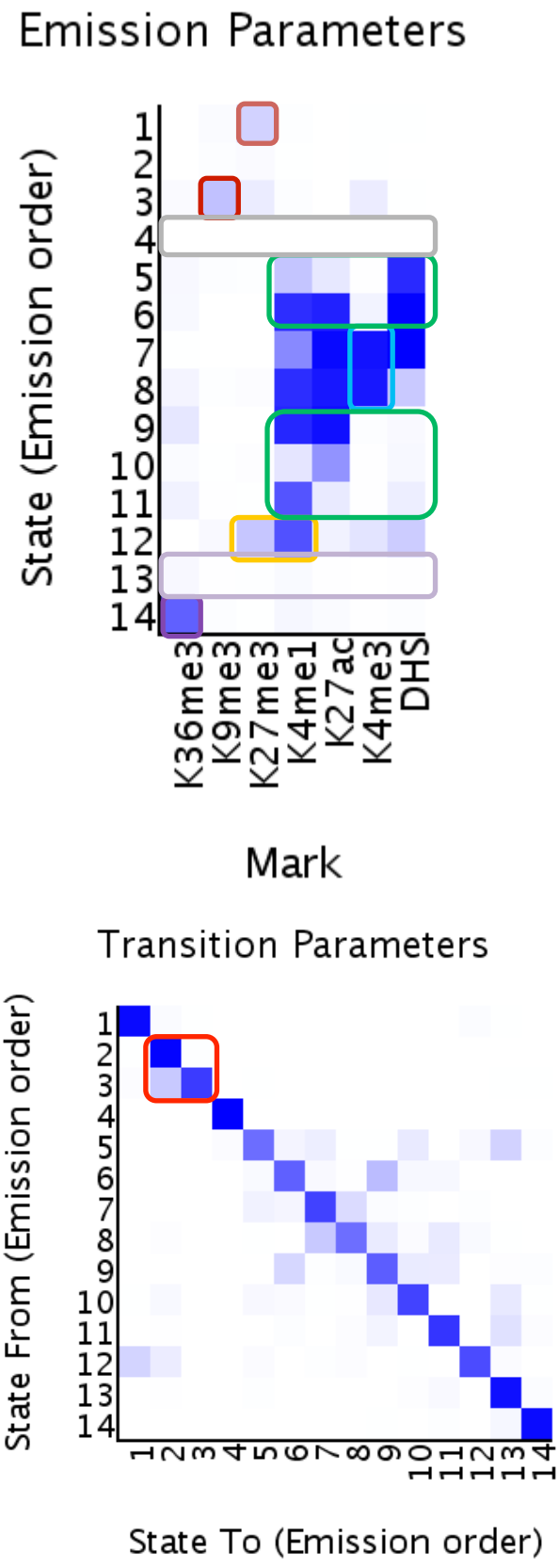

Supp Fig. S3: **B:** correlations between each state in a 20-state model to the most similar state in smaller models, ranging from 5 to 19. Green = highest correlation, Red = lowest correlation. **C:** Calculated from Fig. S3B. For each smaller model, number of states from the 20-state model that are not represented, i.e. that have a correlation of <0.9 or less.

B

state in 20-state model	# states in model: 5	6	7	8	9	10	11	12	13	14	15	16	17	18	19	20
1	0.9990	0.9990	0.9991	0.9991	0.9991	0.9995	0.9992	0.9992	0.9993	0.9994	0.9994	0.9999	0.9999	0.9999	1.0000	1.0000
2	0.9995	0.9996	0.9995	0.9995	0.9994	0.9994	0.9995	0.9995	0.9994	0.9994	0.9994	0.9993	0.9993	0.9993	0.9988	1.0000
3	0.9055	0.9055	0.9288	0.9259	0.9288	0.9640	0.9291	0.9468	0.9446	0.9373	0.9388	0.9339	0.9522	0.9539	0.9963	1.0000
4	0.6831	0.7993	0.8478	0.7961	0.7961	0.8380	0.8443	0.8456	0.8423	0.8442	0.8436	0.9160	0.9179	0.9183	0.9998	1.0000
5	0.8743	0.9494	0.9503	0.9508	0.9507	0.9888	0.9974	0.9972	0.9976	0.9972	0.9973	1.0000	1.0000	1.0000	1.0000	1.0000
6	0.7827	0.7970	0.8240	0.8863	0.8863	0.8645	0.9955	0.9986	0.9996	0.9992	0.9996	0.9999	1.0000	1.0000	1.0000	1.0000
7	0.5866	0.8093	0.8143	0.8168	0.8168	0.8308	0.8339	0.7976	0.7700	0.8402	0.8298	0.8344	0.8232	0.8251	1.0000	1.0000
8	0.7443	0.7659	0.7596	0.7546	0.7547	0.7665	0.7683	0.9855	0.8980	0.9821	0.9952	0.9944	0.9963	0.9960	1.0000	1.0000
9	0.8390	0.9628	0.9587	0.9563	0.9563	0.9511	0.9497	0.9219	0.9565	0.9210	0.9999	0.9999	1.0000	0.9999	1.0000	1.0000
10	0.8790	0.8589	0.8497	0.8604	0.8604	0.9989	0.9989	0.9992	0.9989	0.9994	0.9993	0.9991	1.0000	1.0000	1.0000	1.0000
11	0.6361	0.6588	0.6721	0.6017	0.6023	0.8396	0.9560	0.9751	0.9773	0.9103	0.9352	0.9378	0.9879	0.9879	0.9968	1.0000
12	0.0031	0.1314	0.1347	0.1882	0.1889	0.4520	0.8645	0.8313	0.8228	1.0000	1.0000	0.9999	0.9999	0.9956	0.9999	1.0000
13	0.4384	0.4726	0.4837	0.6529	0.6535	0.7472	0.8446	0.8085	0.8067	0.8915	0.8645	0.8627	0.9999	0.9999	1.0000	1.0000
14	0.5316	0.8485	0.8562	0.8619	0.8618	0.8596	0.8599	0.9393	0.9989	0.9402	0.9983	0.9982	0.9992	0.9992	1.0000	1.0000
15	0.9721	0.9792	0.9807	0.9937	0.9937	0.9967	0.9977	0.9988	0.9991	0.9982	0.9985	0.9996	0.9999	0.9999	1.0000	1.0000
16	0.8014	0.8223	0.8311	0.8585	0.8579	0.8613	0.8741	0.8798	0.8673	0.8660	0.8669	0.8615	0.8627	0.8629	0.8619	1.0000
17	0.7998	0.8294	0.8554	0.8737	0.8730	0.8525	0.8818	0.8722	0.9988	0.9714	0.9761	0.9803	0.9994	0.9880	0.9998	1.0000
18	0.9871	0.9872	0.9886	0.9888	0.9996	0.9996	0.9996	0.9995	0.9995	1.0000	1.0000	1.0000	1.0000	0.9993	1.0000	1.0000
19	0.9816	0.9815	0.9801	0.9802	0.9998	0.9993	0.9998	0.9999	0.9994	0.9999	1.0000	1.0000	0.9999	0.9931	0.9999	1.0000
20	0.6391	0.6434	0.6547	0.6538	0.9986	0.9993	0.9986	0.9983	0.9994	0.9999	0.9998	0.9999	0.9999	0.9982	1.0000	1.0000

C

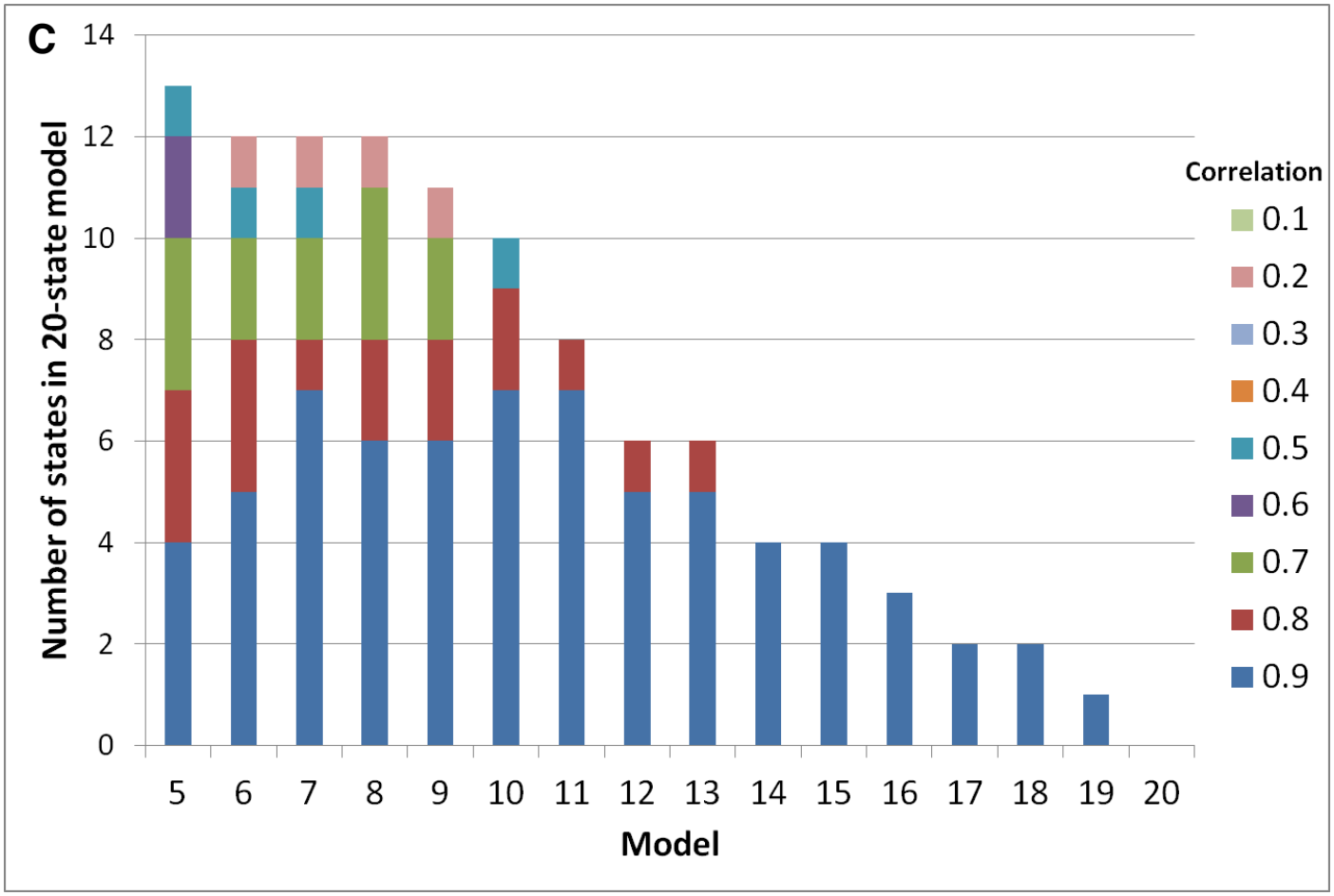

Supp Fig. S4A – Chromatin environments at sex-independent DHS in male and female liver. Chromatin states (*top*) and chromatin mark read densities (*bottom*). Chromatin states are numbered per the color bars at *right*.

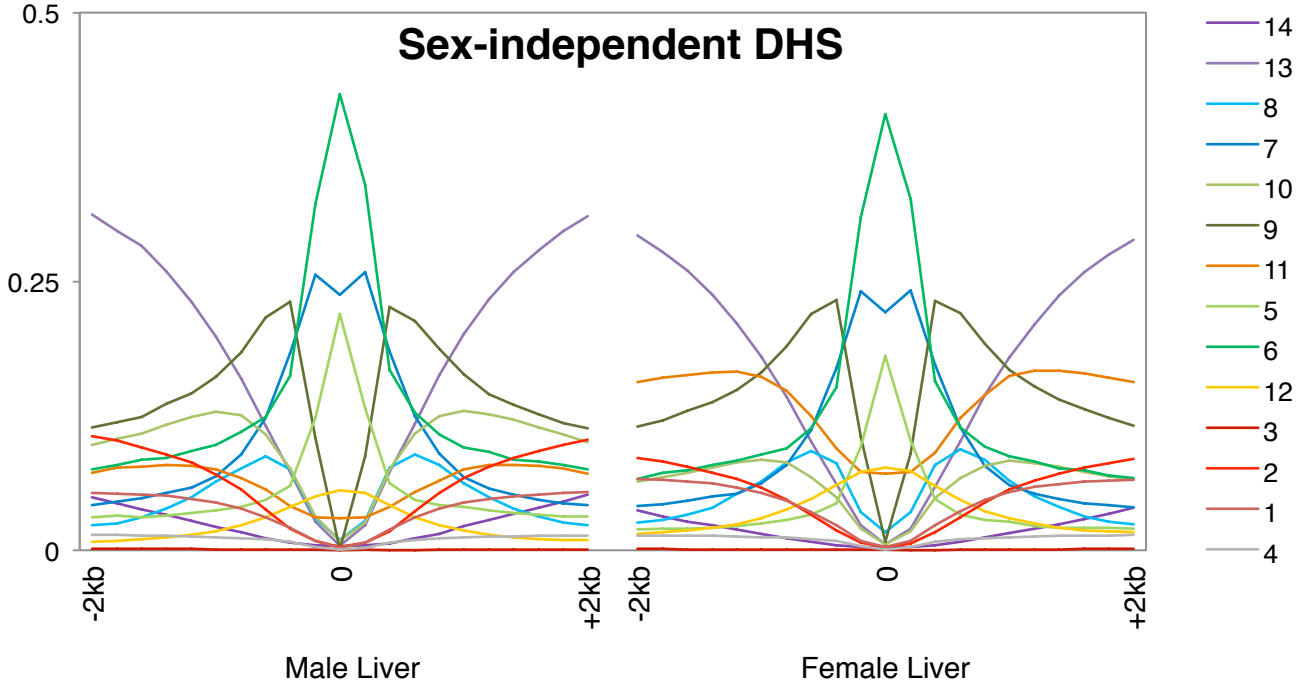

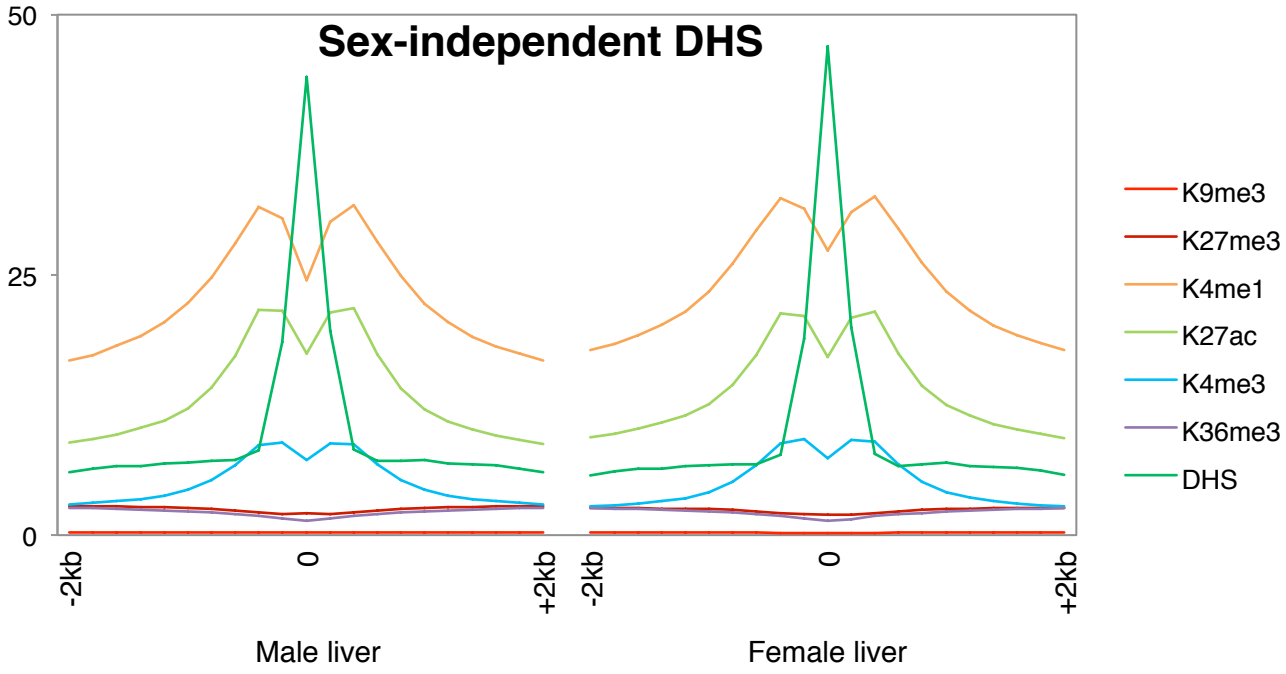

Supp Fig. S4B – Chromatin environments at sex-biased DHS in male and female liver. Chromatin states at male-biased DHS (*top*) and female-biased DHS (*bottom*) in male liver (*left*) and female liver (*right*).

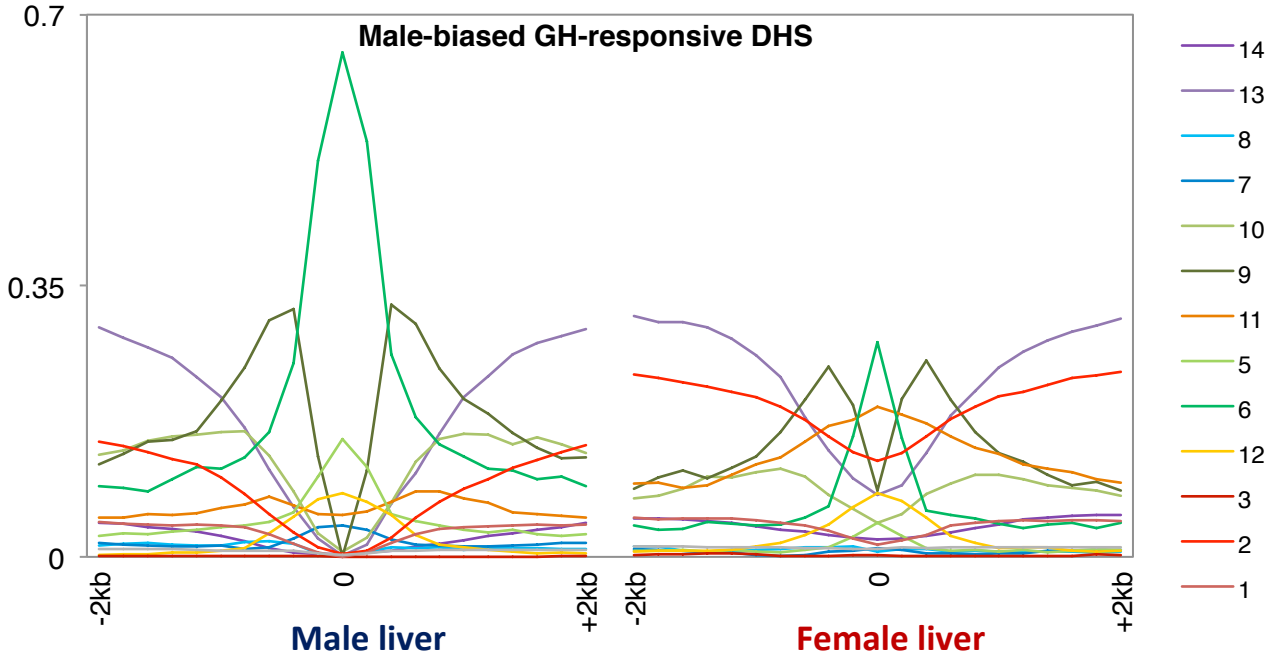

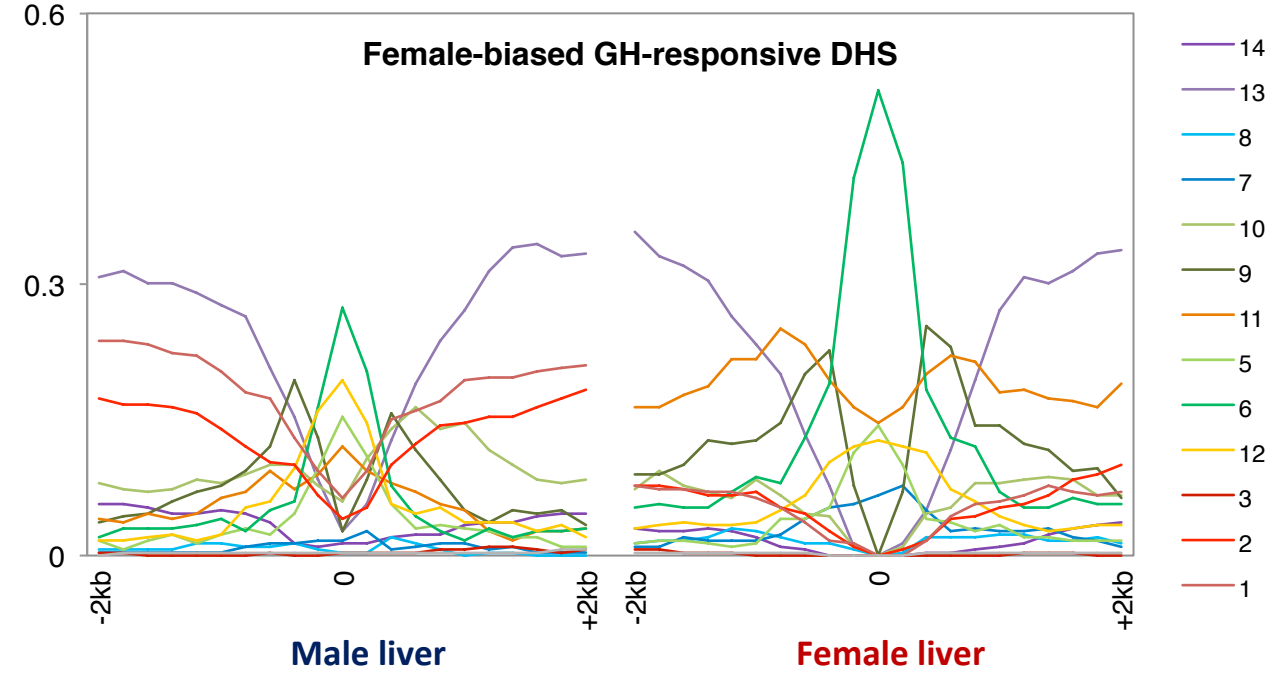

Supp Fig. S4C – Chromatin state environments at sex-independent TSS (*top*) and sex-biased TSS (*middle* and *bottom*).

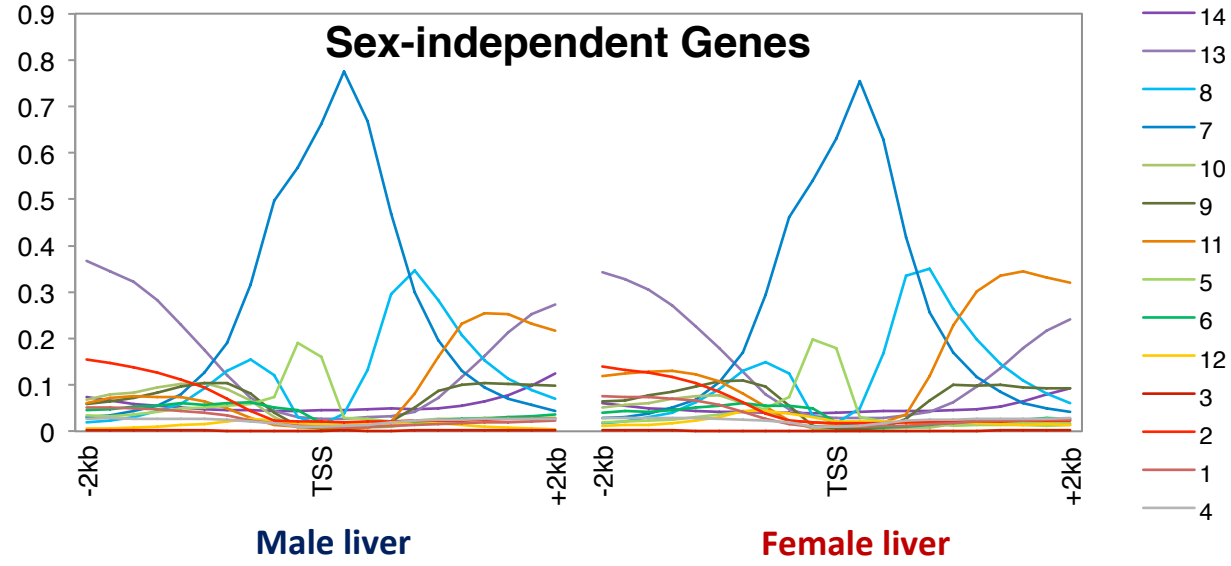

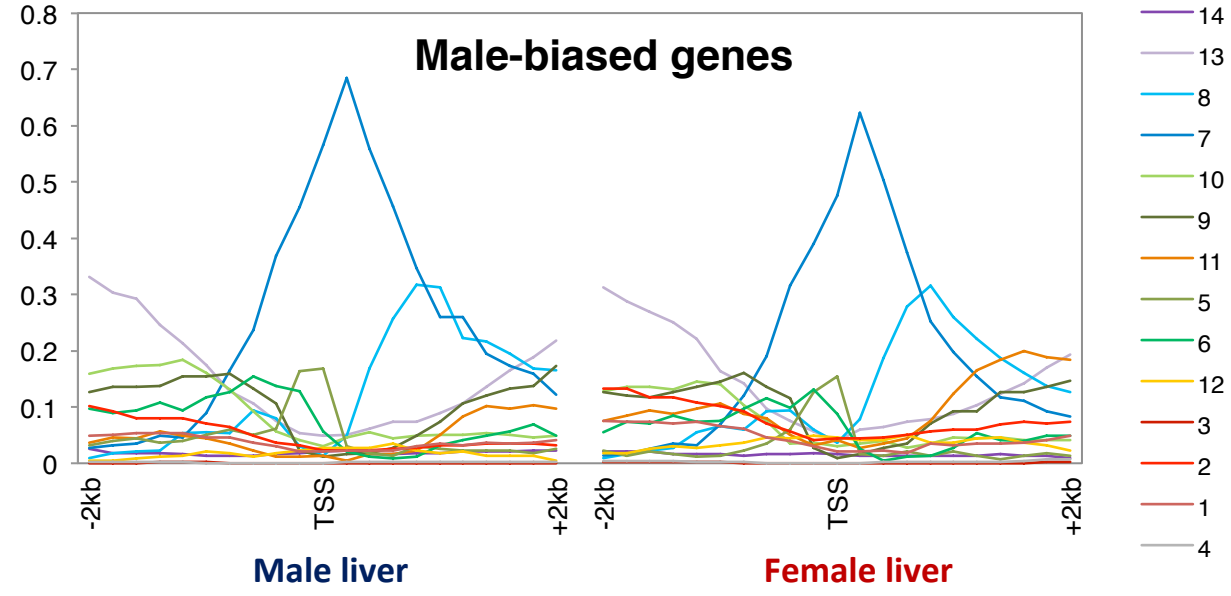

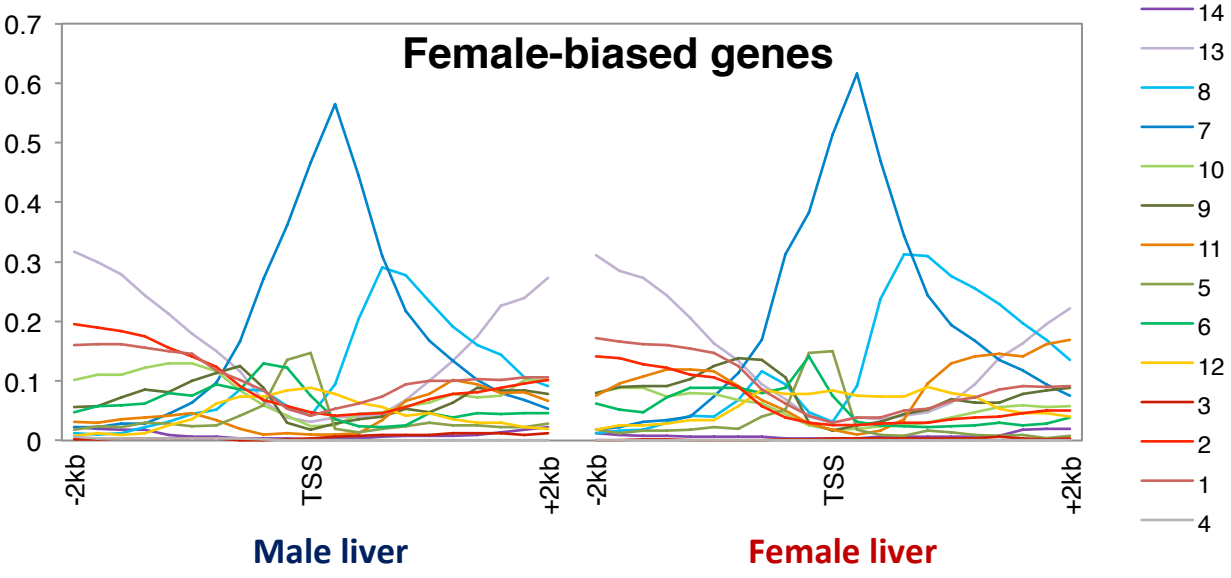

Supp Fig. S5: Genes clustered by chromatin mark read densities surrounding TSS and TES. **A**: Heat map for 15,533 liver-expressed and non-liver-expressed genes clustered by chromatin read densities in 200-bp non-overlapping windows within 2 kb regions surrounding the TSS and TES, with cluster numbers given on the *left*. K9me3 is largely absent from the six gene clusters obtained, as it is primarily found in intergenic regions (Fig. S2). Genes in cluster 1 are distinguished by high density K4me1, K27ac, and DHS reads around both the TES and the TSS. Thus, cluster 1, but not clusters 2 and 3, exhibits active enhancer states around the TES (c.f., Fig. 3A). Cluster 2 genes show a more symmetrical distribution of marks around the TSS than the other two active clusters, clusters 1 and 3. **B:** Percentage of genes in each cluster that are expressed in liver (log2 RPKM>=1) or are not expressed in liver. **C:** % of the gene body covered by a DHS domain (SICER island), for each of the 6 clusters. **D**: % of genes in each cluster for which at least 50% of the gene body is covered by a SICER island. DHS islands are from Ling *et al.*, Molec Cell Biol 2010.

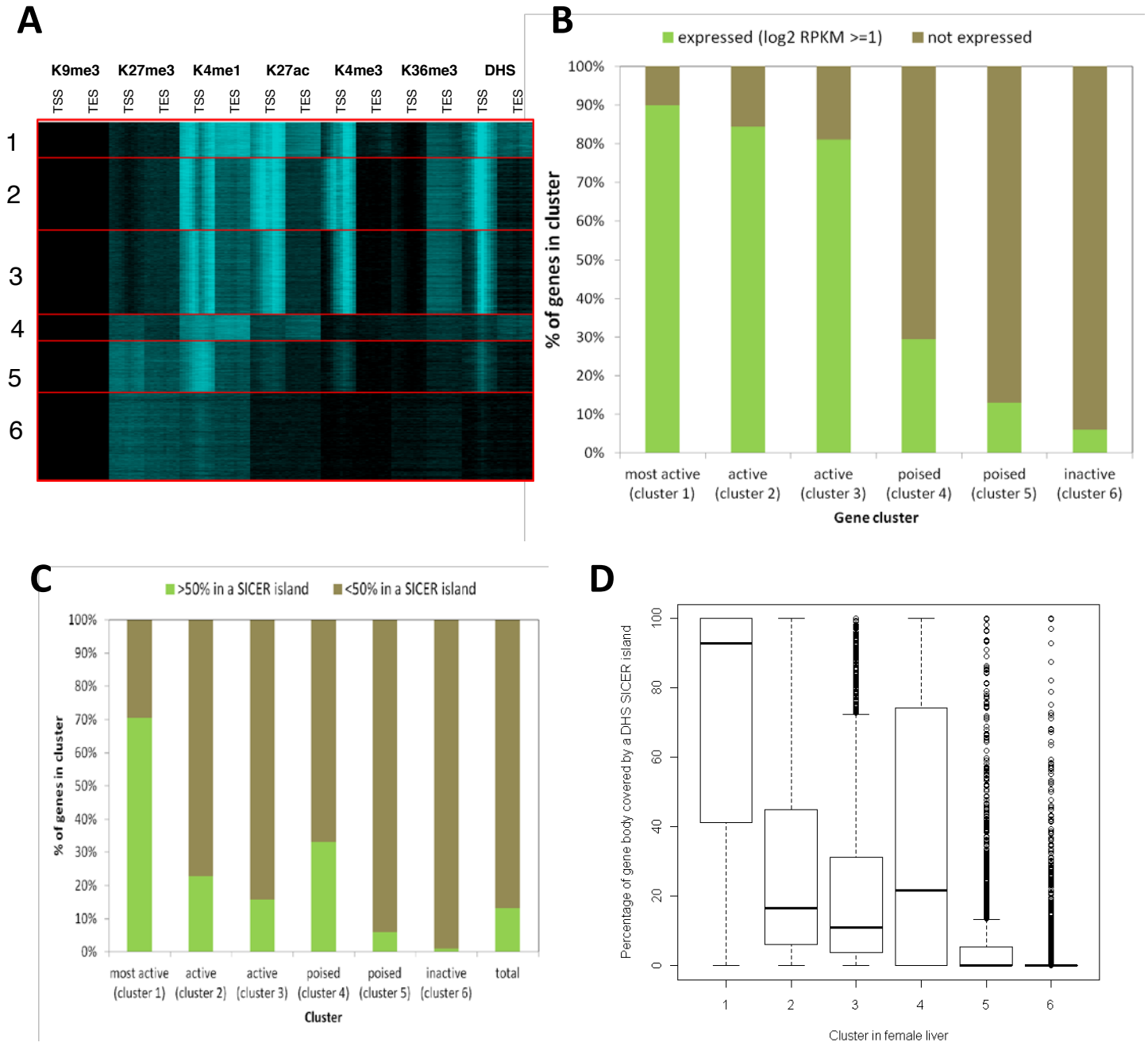

Supp Fig. S6: Sex-biased genes clustered by chromatin mark density.

Both sets of sex-biased genes were clustered separately in male and female liver by read densities in TSS +/- 1 kb and TES +/- 1 kb. (**A**) Heat maps of clusters

A

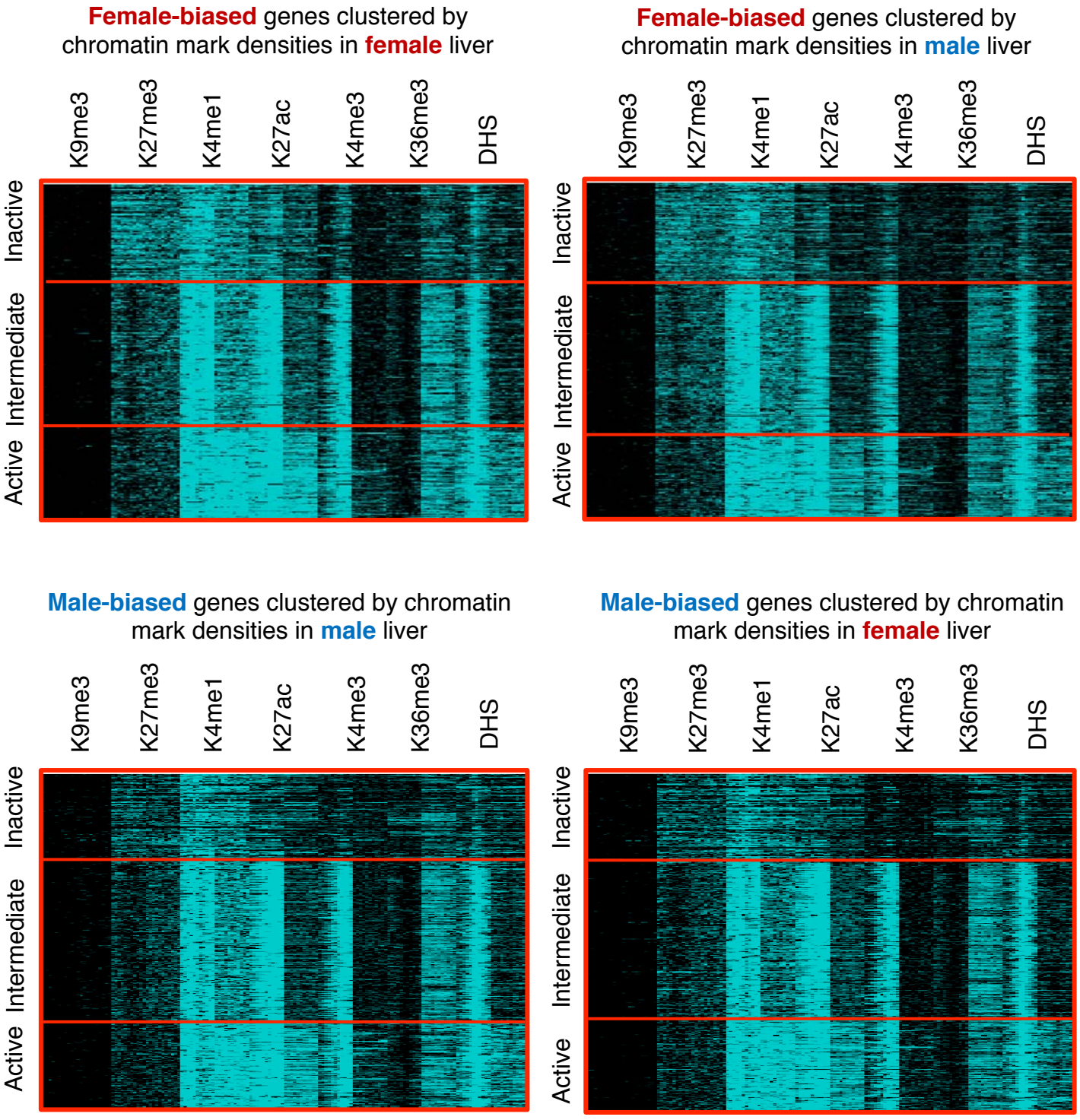

Supp Fig. S6: Sex-biased genes clustered by chromatin mark density.

(**B**) read density profiles and chromatin state profiles, for female-biased genes clustered in female liver

B

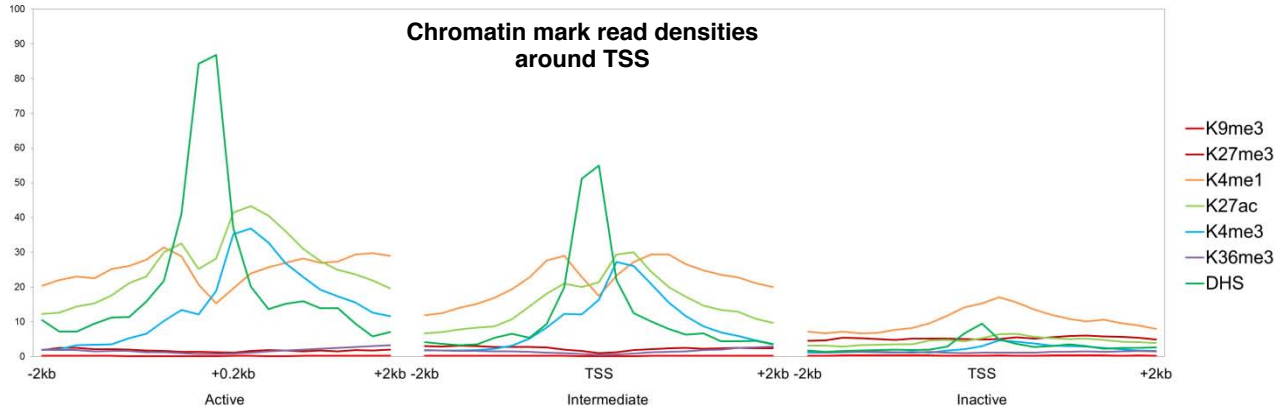

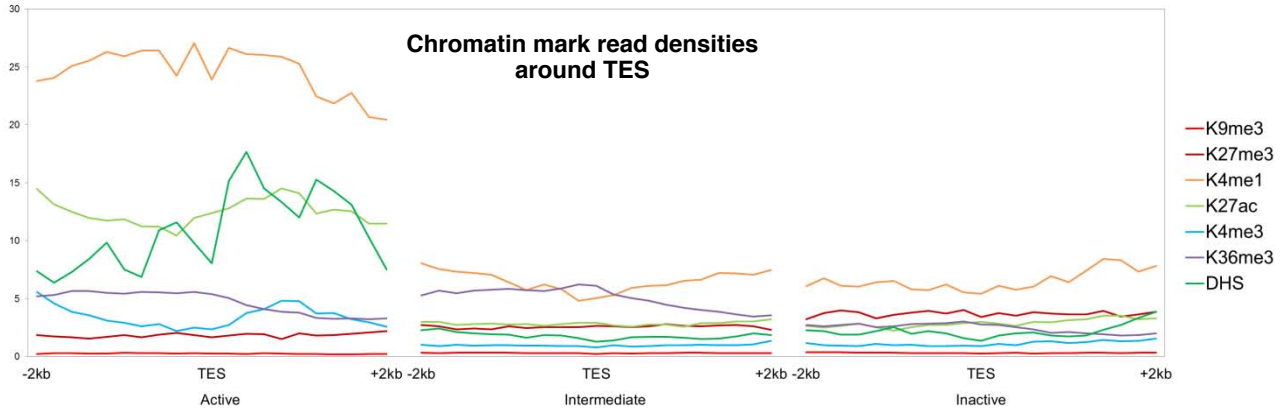

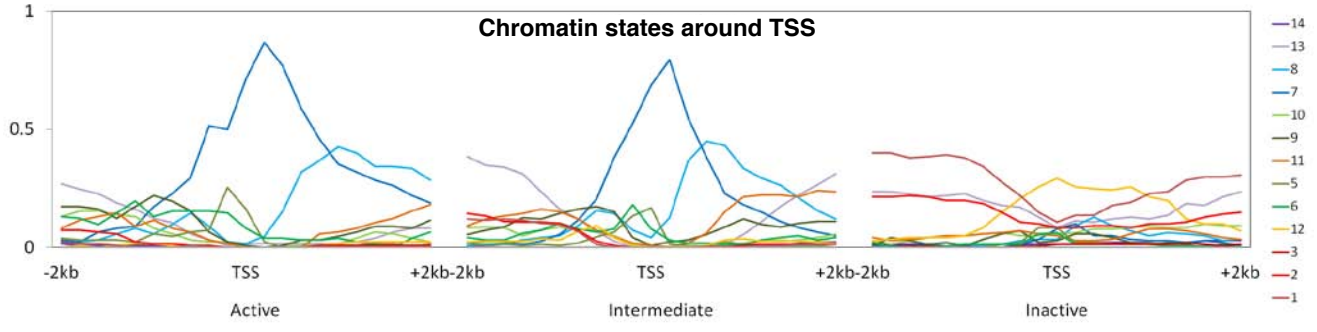

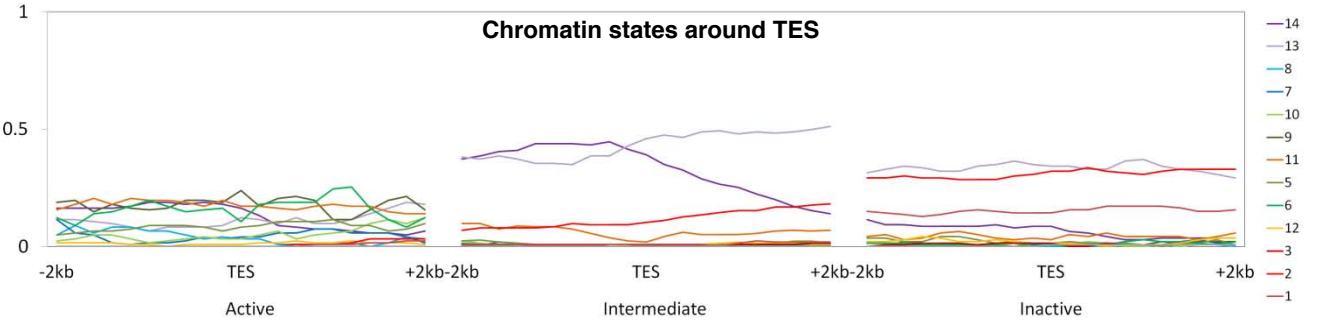

Supp Fig. S6: Sex-biased genes clustered by chromatin mark densities, continued. **C.** gene expression for genes in each cluster in livers of each sex**. D:** Correspondence between sex-biased gene clusters and all-gene clusters for male-biased genes in male liver and for female-biased genes in female liver

C

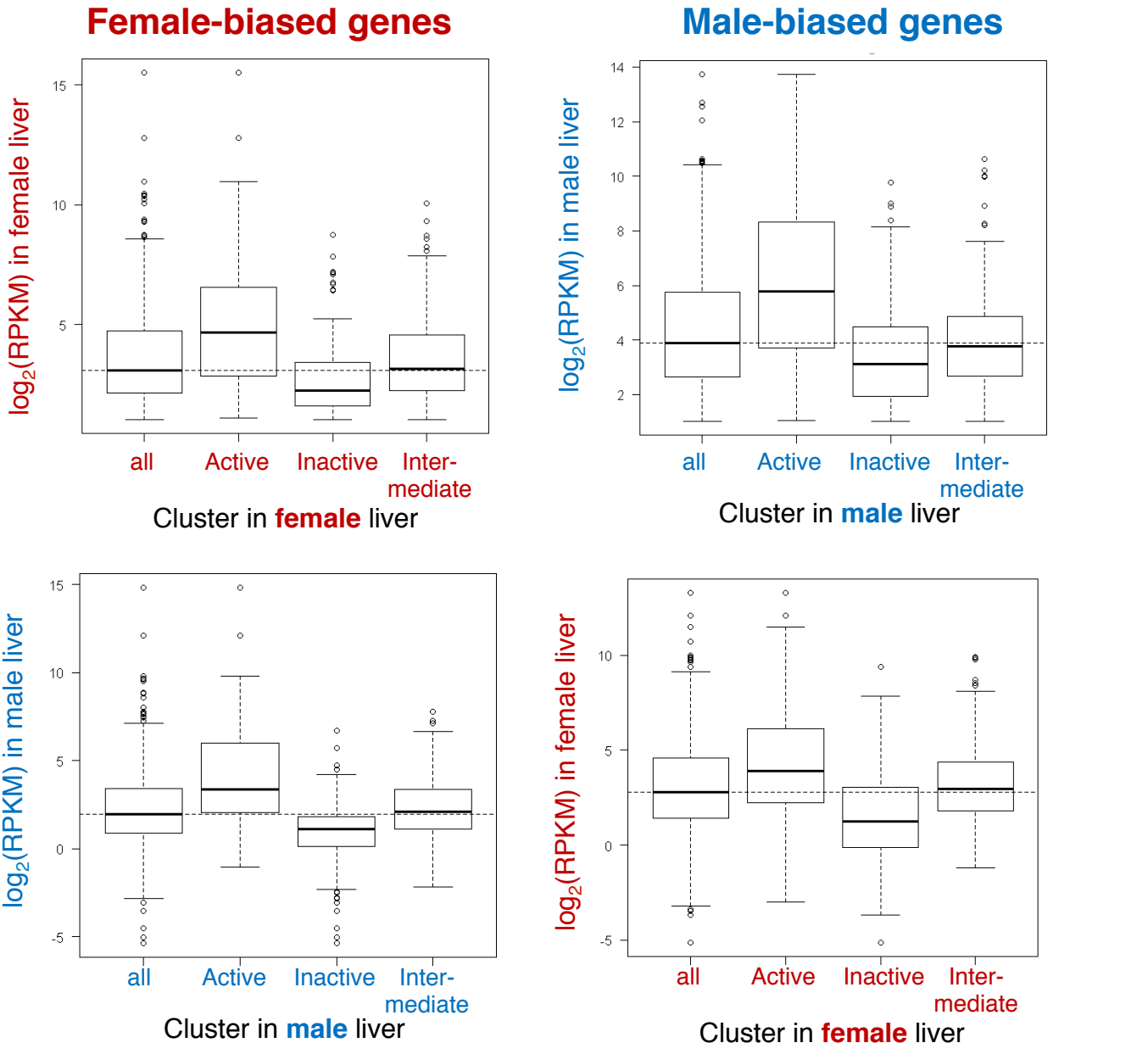

D

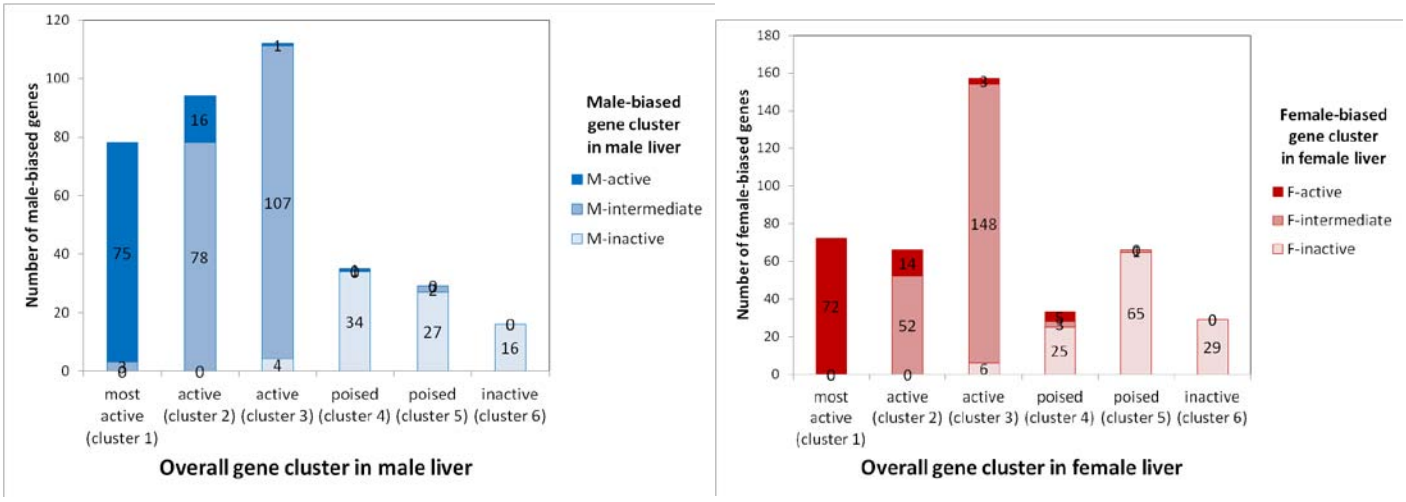

Supp Fig. S6: Sex-biased genes clustered by chromatin mark densities, continued. **E.** Chromatin marks identified using MACS/SICER associated with each class of female-biased (*top*) and male-biased (*bottom*) gene, along with the sex-specificity of each chromatin mark. "none", no MACS or SICER-identified mark associated with the promoter (K4me3) or gene body (all other modifications). *, chromatin marks for which the distribution of (male, female, sex-independent, none) for that category of genes is significantly different from that for the set of all male-biased or all female-biased genes ($p<0.05$; Chi-square test). **F:** Fraction of sex-biased genes that lack a sex-biased chromatin mark up to 100 kb from the gene body.

E

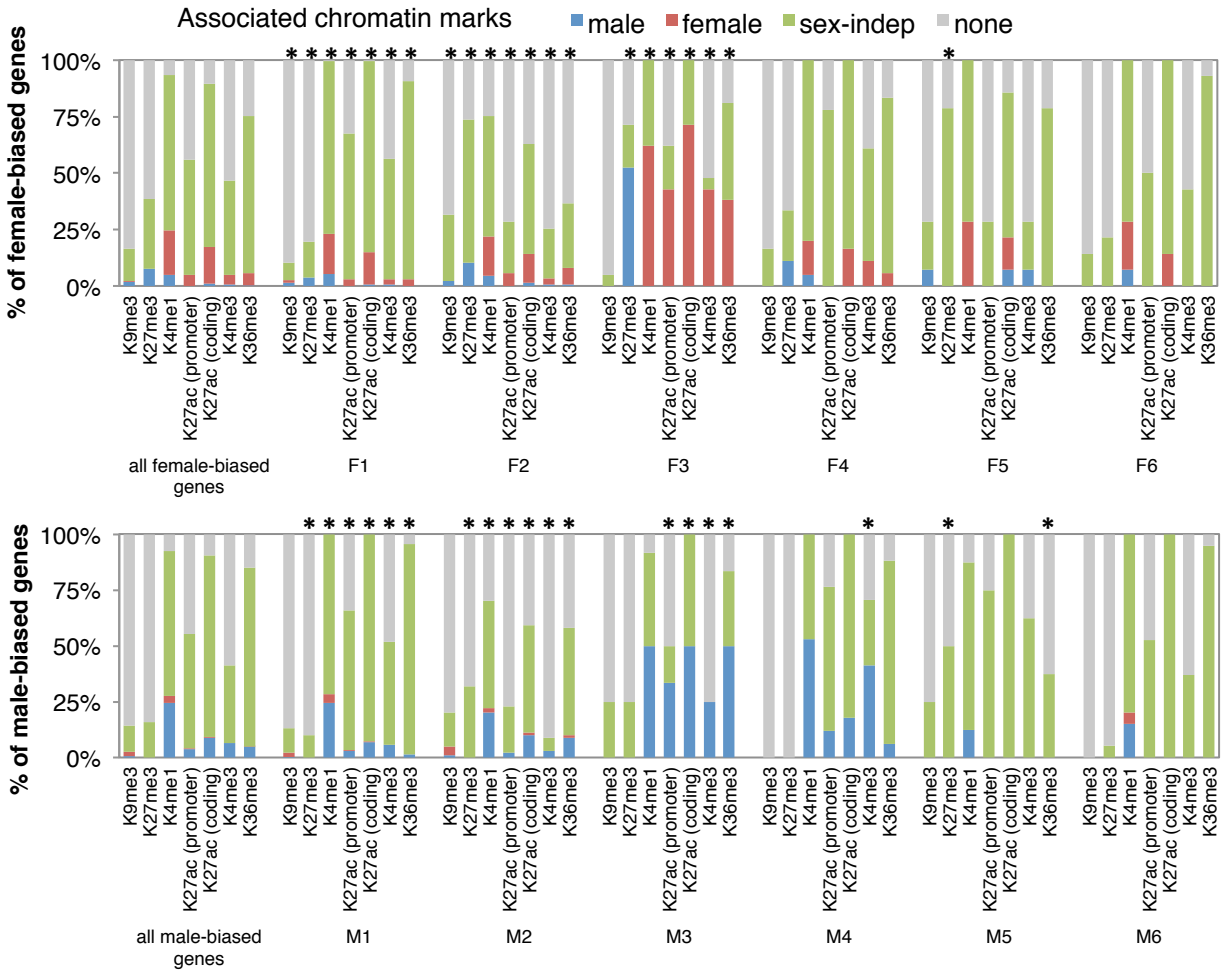

F

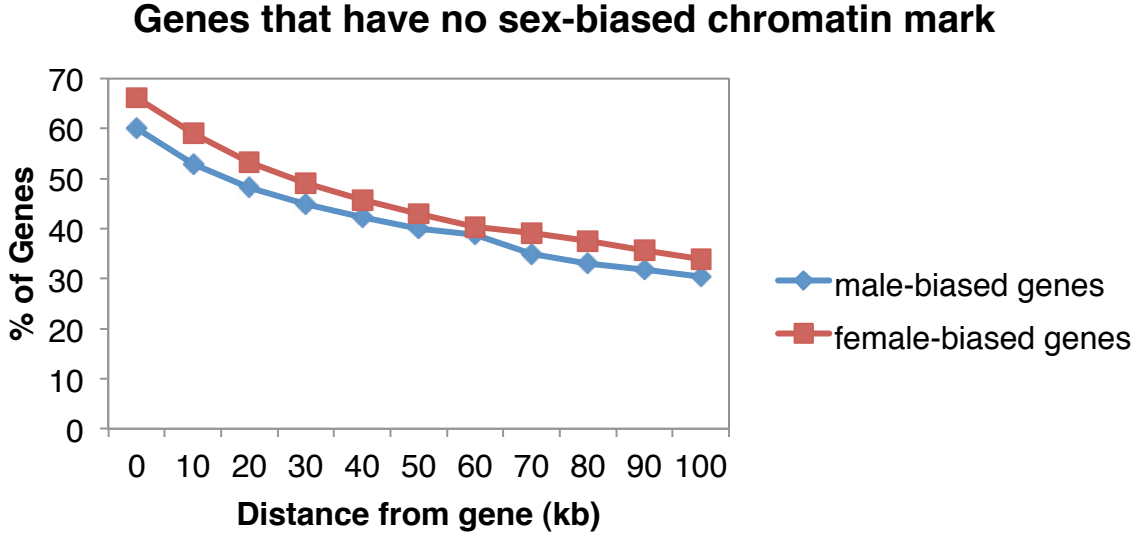

Supp Fig. S6G Gene expression (log_2(RPKM) of sex-biased genes in each class.

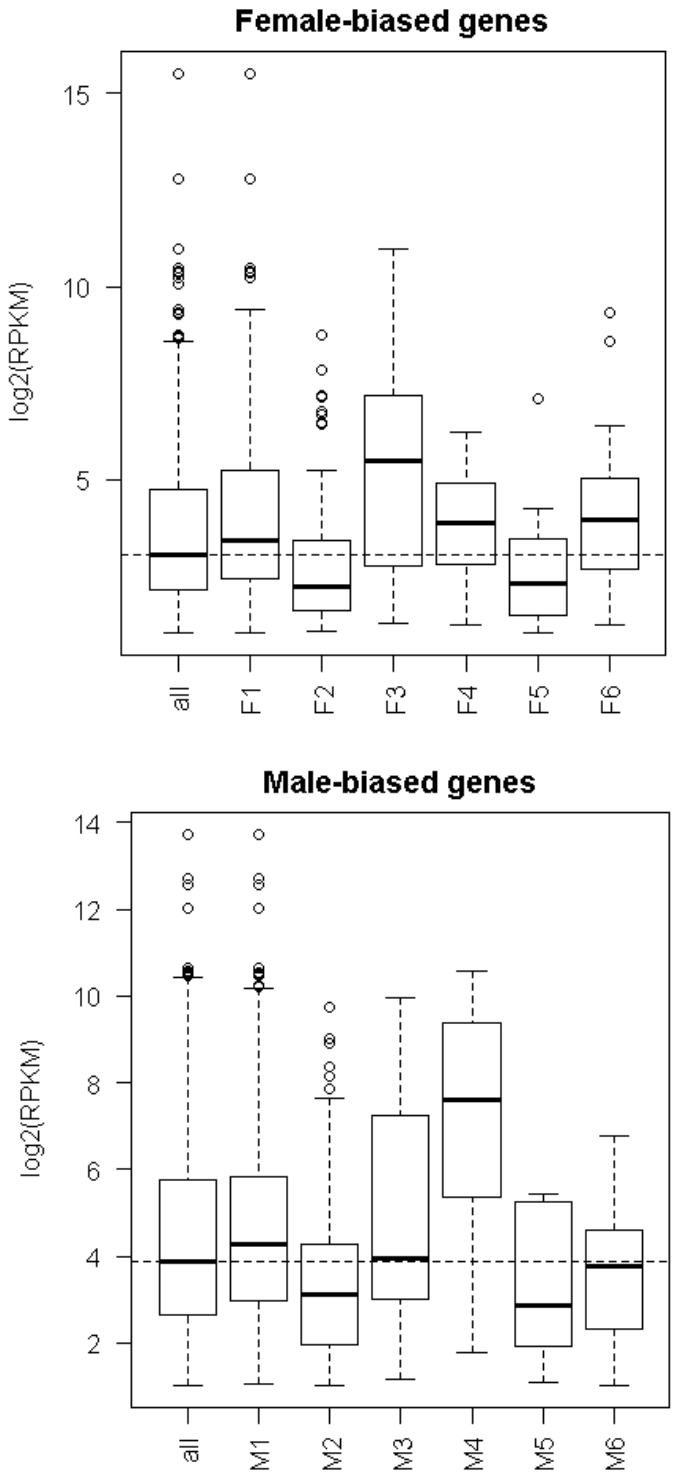

Supp Fig. S7: Sex-biased genes grouped by sex-ratio in gene expression.

Female-biased genes were ranked by gene expression ratio and divided into four groups by gene expression ratio, with 118-121 genes in each group. Male-biased genes were similarly divided into four groups, with 103-108 genes in each group. **A**: Chromatin marks identified using MACS/SICER associated with each quarter of female-biased (*top*) and male-biased (*bottom*) gene, along with sex-specificity of each chromatin mark. "none", no MACS or SICER-identified mark associated with the promoter (K4me3) or gene body (all other modifications). Only a small fraction of sex-biased genes overall have sex-biased local chromatin marks, and male-enriched K27me3 is seen at 25% of the most highly female-biased genes, but there are no male-biased genes with female-enriched K27me3.

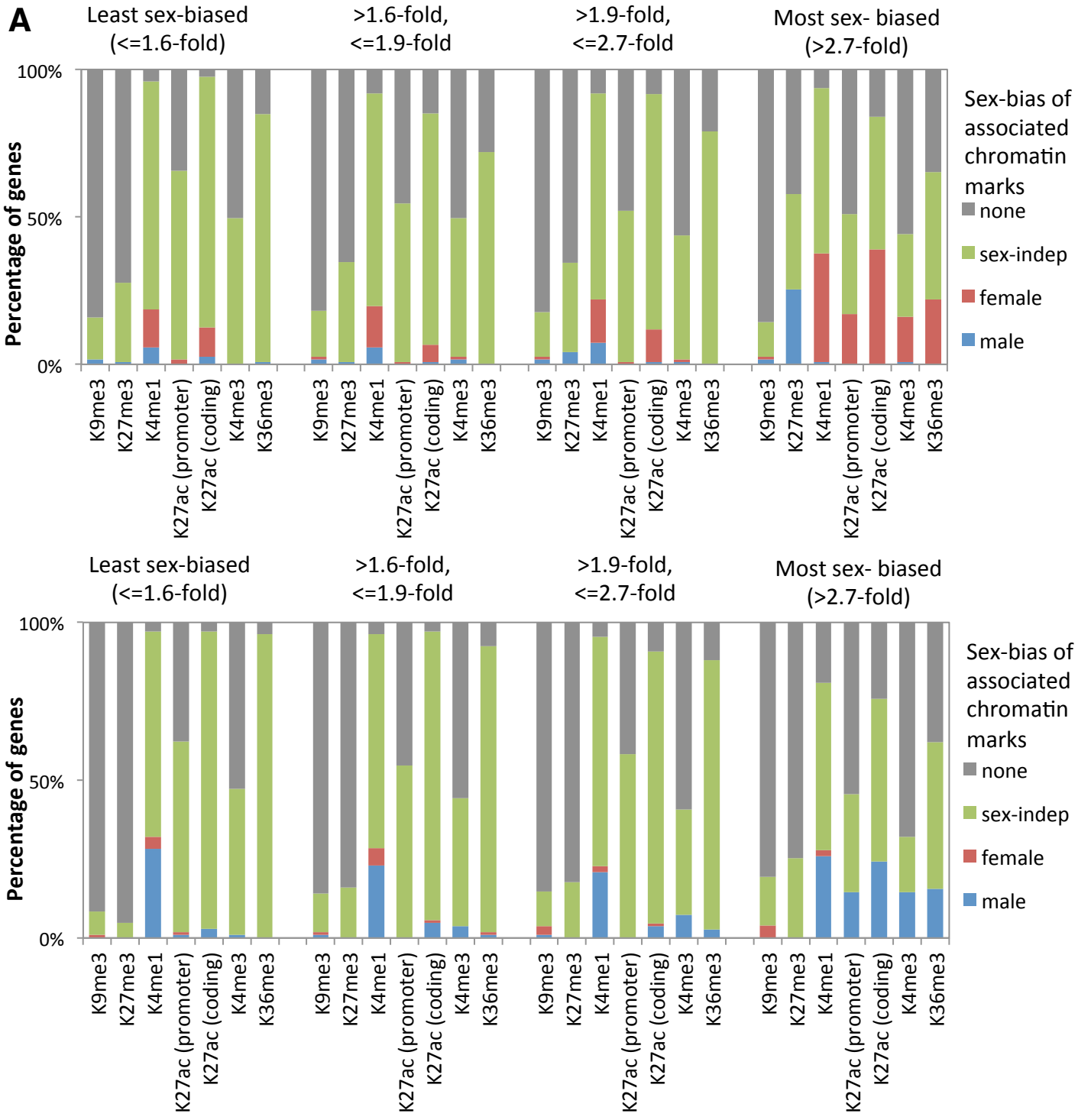

Supp Fig. S7: Sex-biased genes grouped by sex-ratio in gene expression.
Female-biased genes were ranked by gene expression ratio and divided into four groups by gene expression ratio. Male-biased genes were similarly divided into four groups. **B:** Fold enrichment for each group of female-biased (*top*) or male-biased genes (*bottom*) that are targets of a particular TF (i.e., within 10 kb of a TF binding site), compared to the background of all liver-expressed genes. Data is shown for enrichments that meet $p<0.05$. Since each quarter contains equal numbers of genes, enrichments are not biased by the numbers of genes in each group. **For female-biased genes**, The TFs that preferentially target genes exhibiting sex-differences in local chromatin (class F3; Fig. 5A) also preferentially target the most highly female-biased genes (top panel), consistent with F3 genes collectively showing the greatest sex-differences in expression (Fig. 4B, left). **For male-biased genes**, there is not a clear relationship between sex-differences in chromatin marks at a gene and magnitude of sex-bias in gene expression. E.g., CUX2 targets are most highly enriched among M4 genes, which exhibit sex-differences in local chromatin marks (Fig. 5A), but CUX2 does not have a preference for genes that are highly male-biased in expression (bottom panel). This is consistent with M4 not containing the most highly male-biased genes (Fig. 4B, right).

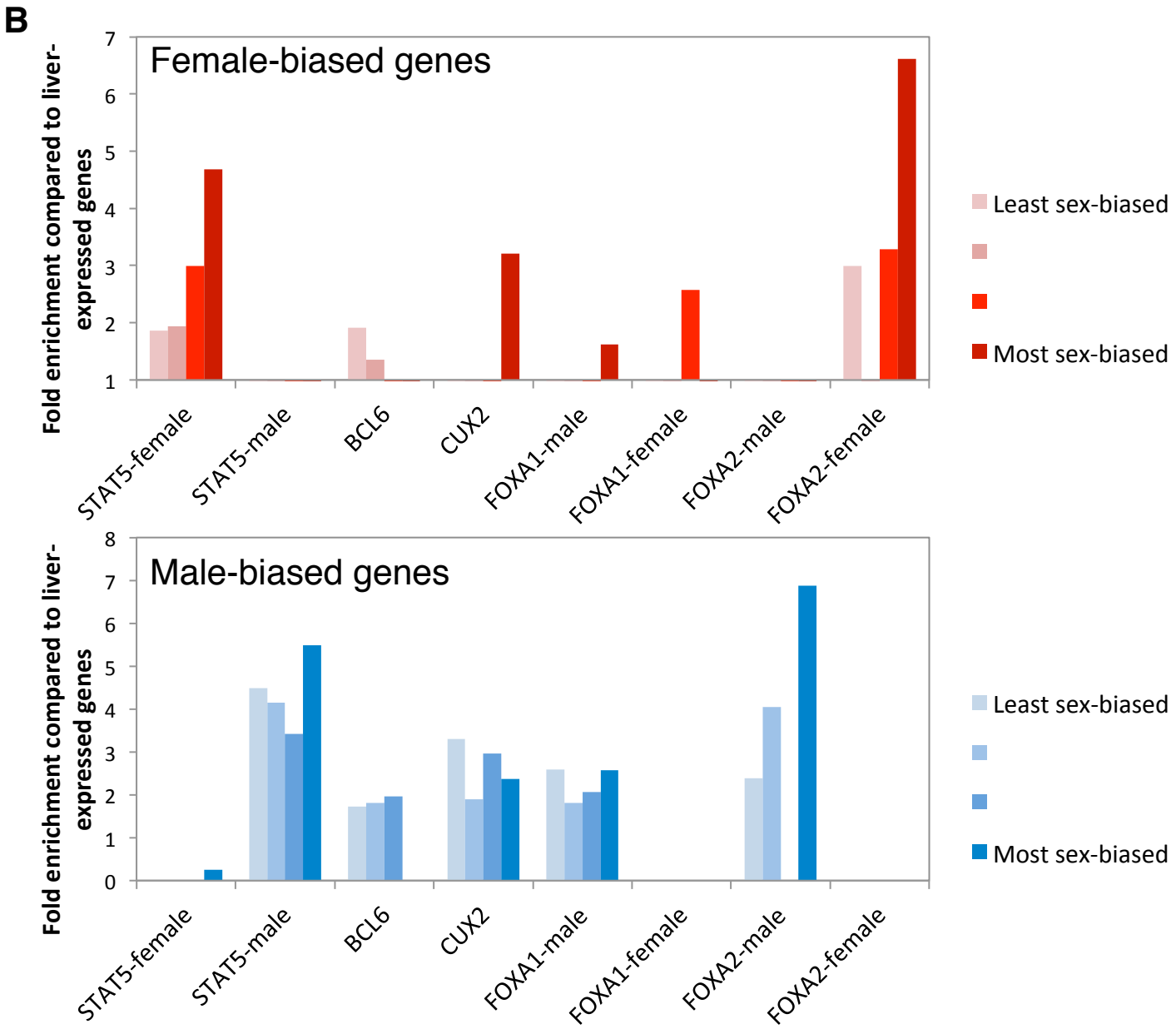

Supp Fig. S8. **A-H**: Fractions of ChIP-seq determined TFBS that occur at DHS in bins of 1000 DHSs each, ranked by M/F ratio in DNase hypersensitivity (blue), K4me1 (purple), K27ac (green), and K27me3 (red). On the x-axis in each panel are ranked DHS bins with high M/F ratio (male-bias) towards the left and low M/F ratio (female-bias) towards the right. The y-axis indicates the fraction of binding sites of (**A**) male-enriched STAT5, (**B**) female-enriched STAT5,(**C**) male-enriched FOXA2, (**D**) female-enriched FOXA2, (**E**) male-enriched FOXA1, (**F**) female-enriched FOXA1, (**G**) BCL6 in male, and (**H**) CUX2 in female. **I:** Fractions of male-enriched, female-enriched, and sex-independent STAT5 binding sites that overlap a sex-independent or sex-biased FOXA binding sites. Consistent with female-enriched STAT5-binding sites being relatively open in both male and female liver (Zhang et al 2012), female-enriched STAT5 binding sites are more likely than male-enriched STAT5 binding sites to coincide with a sex-independent FOXA, especially FOXA1, binding site.

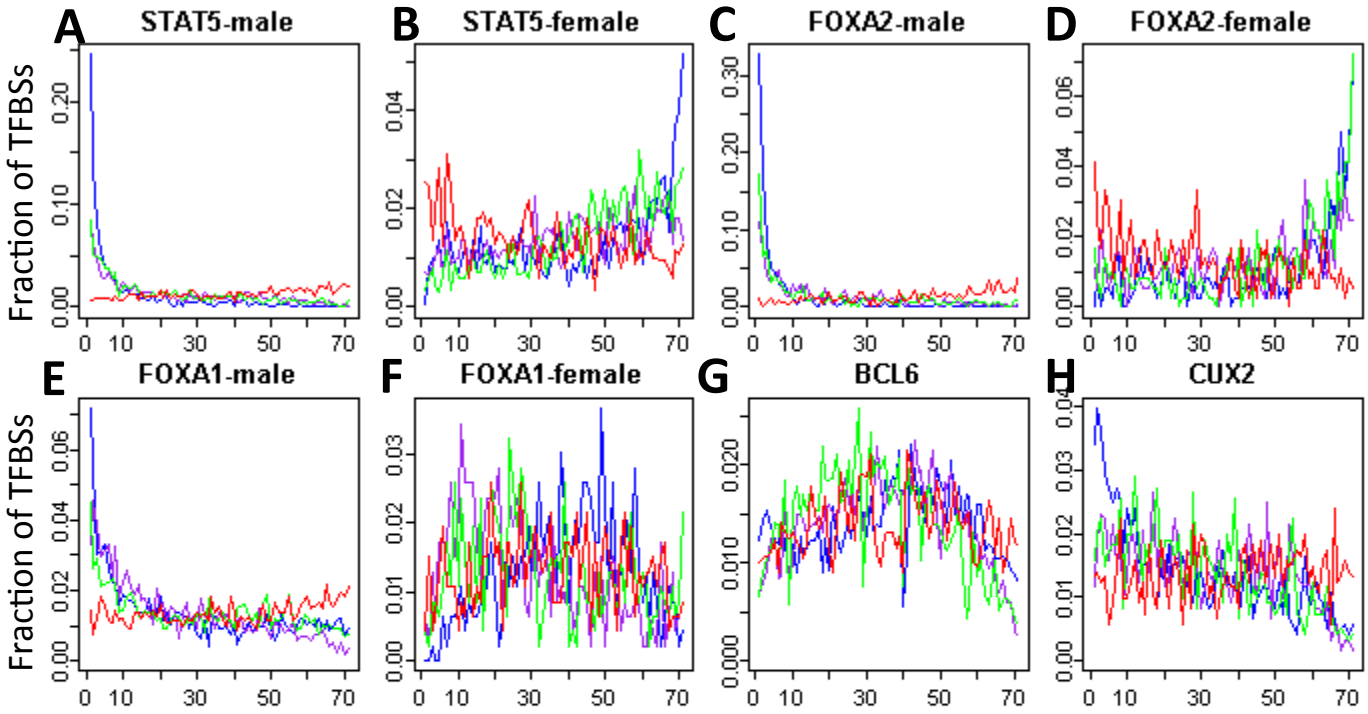

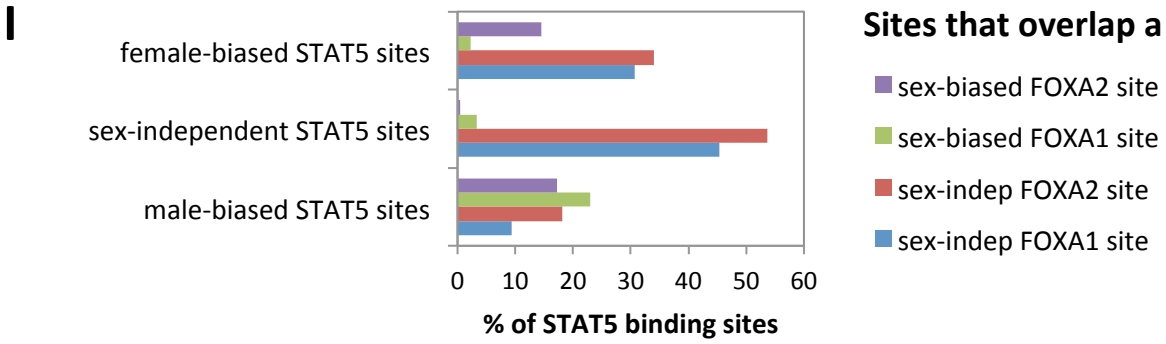

Supp Fig. S9 Legend. Scatter plots of sex-ratios in DNase hypersensitivity, K4me1, K27ac, and K27me3 (left to right) on the y-axis and sex-ratios in STAT5, FOXA1, and FOXA2 binding (**A-C**) and BCL6 and CUX2 binding intensity (**D** and **E**) on the x-axis. Pearson correlations with p-values are shown in top left of each panel.

For FOXA1, FOXA2 and STAT5, male-enriched binding sites are shown in blue, female-enriched binding sites in red, and sex-independent in black. For FOXA1, there are very few female-enriched binding sites, which results in curved plots, especially in relation to DNase hypersensitivity (Fig B, left-most panel) where there is a relationship for male-enriched sites but not for female-enriched sites. For BCL6 and CUX2, green line shows linear regression line. For BCL6 no relationships are seen, but for CUX2, there is some correlation between CUX2 binding intensity and male-bias in DNase hypersensitivity.

Supp figure S9 A-E

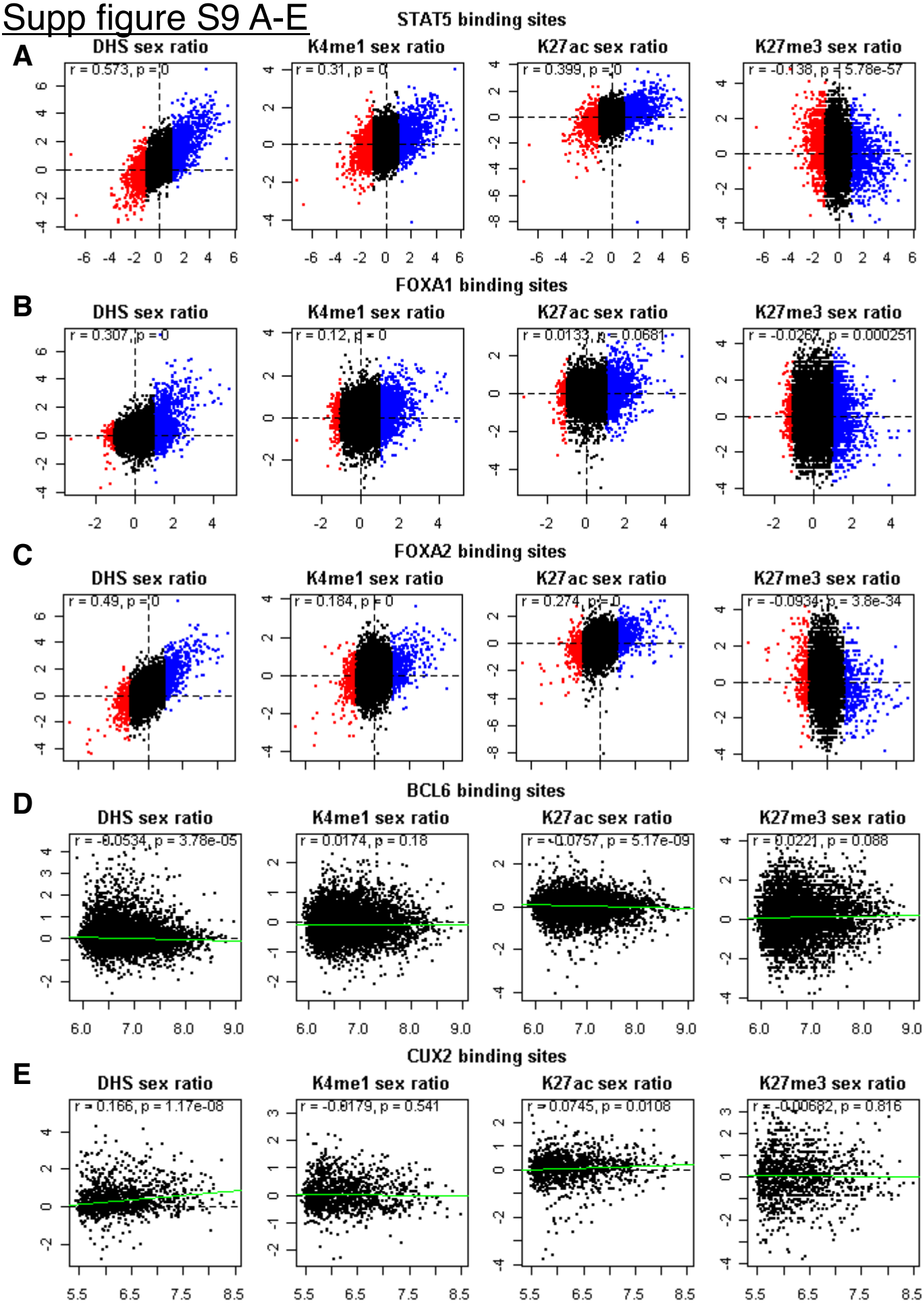

Supp Fig. S10 **A-C -** K4me1 read profiles at sex-biased DHS sites. In each panel, the K4me1 profile in male liver is shown in blue and female liver in red. Read counts are normalized to the total number of DHS in each panel. **A:** male-biased DHSs and STAT5 binding. **B**: Male-biased DHSs male-enriched STAT5 binding, with and without male-enriched FOXA2 binding (*top*) or CUX2 binding in female *(bottom*). **C**: Female-biased DHSs and STAT5 binding. The differences are quantified in Supp Fig S10 D-E.

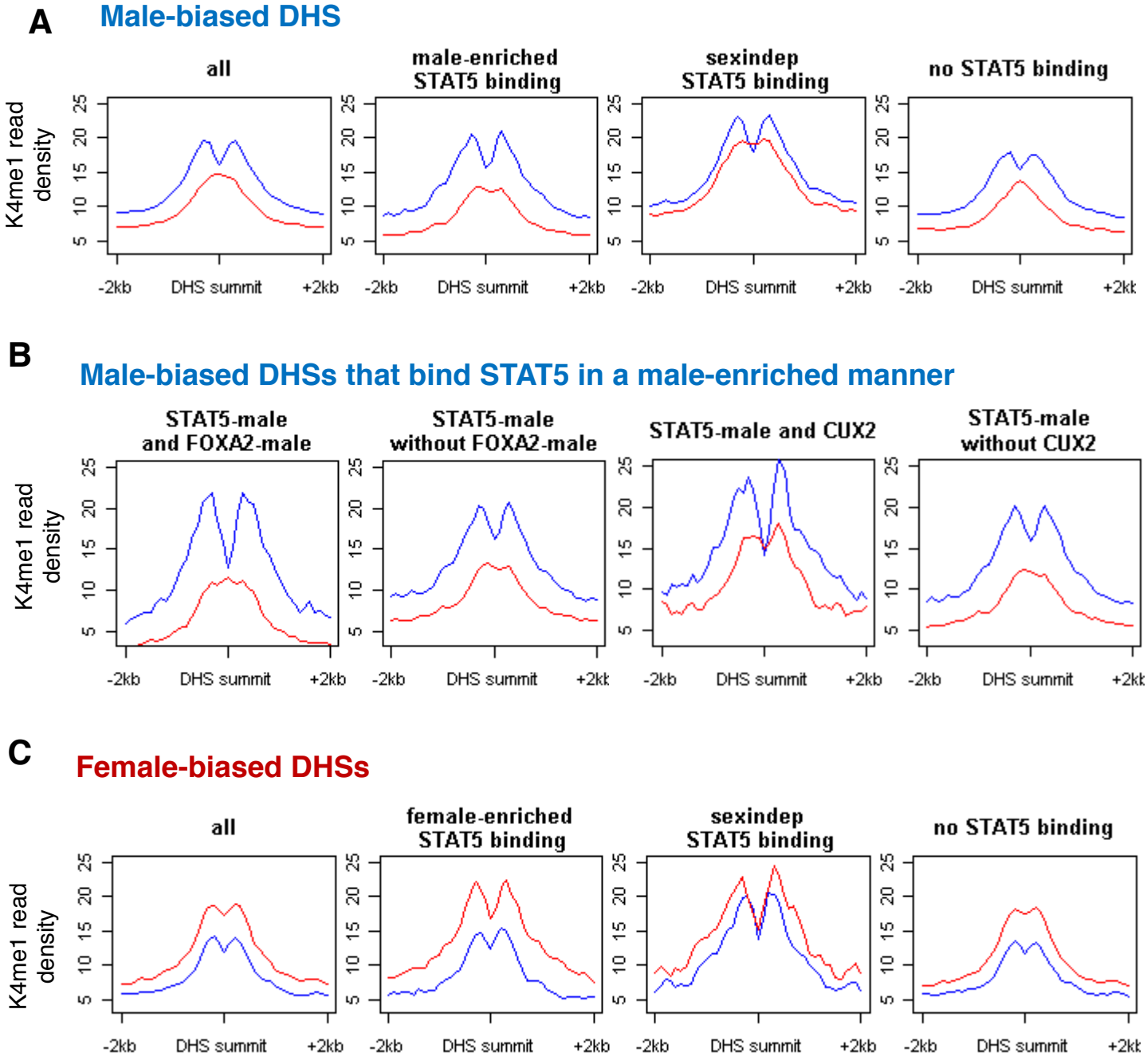

Supp figure S10 **D-E** Difference between K4me1 reads at DHS summit and K4me1 peak, in male liver and female liver for male-biased and female-biased DHSs with or without FOXA1 or FOXA2 binding. For male-biased DHSs, the column on the left lists the K4me1 read count at the DHS peak summit subtracted from the read count at the highest point for K4me1, in male liver. The next column lists the corresponding value in female liver, and the third column is the difference between the two : $[(\text{K4me1 max} - \text{DHS summit})_{male} - (\text{K4me1 max} - \text{DHS summit})_{female}]$.

D

	Male-biased DHSs				Female-biased DHSs			
	K4me1 trough depth		Difference between Male and Female		K4me1 trough depth		Difference between Female and Male
	Male liver	Female liver			Female liver	Male liver	
all male-biased DHS	3.62	-1.10	4.72	all female-biased DHS	1.75	2.12	-0.38
FOXA2 (male)	6.14	-1.70	**7.83**	FOXA2 (female)	2.44	1.19	**1.25**
FOXA2 (sexindep)	6.64	0.80	5.84	FOXA2 (sexindep)	4.06	3.58	0.48
no FOXA	2.49	-1.48	**3.84**	no FOXA2	1.02	1.63	**-0.61**
all male-biased DHS	3.62	-1.10	4.72	all female-biased DHS	1.75	2.12	-0.38
STAT5 (male)	5.26	0.07	**5.19**	STAT5 (female)	5.56	2.39	**3.17**
STAT5 (sexindep)	5.47	0.42	5.04	STAT5 (sexindep)	9.26	6.69	2.58
no STAT5	2.54	-1.45	**4.00**	no STAT5	0.91	1.63	**-0.73**
all male-biased DHS	3.62	-1.10	4.72				
FOXA1 (male)	7.34	-0.10	**7.44**				
FOXA1 (sexindep)	7.18	0.69	6.49				
no FOXA	2.44	-1.45	**3.84**				

E

pairs of TFs at male-biased DHSs	...with FOXA1-male	...without FOXA1-male	...with FOXA2-male	...without FOXA2-male	...with STAT5-male	without STAT5-male	...with CUX2	...without CUX2
FOXA1-male			7.95	7.17	9.75	6.56	10.91	7.92
FOXA2-male	7.95	7.05			9.67	6.81	14.75	6.81
STAT5-male	9.75	3.82	9.67	4.26			8.46	4.74
CUX2	10.91	7.92	14.75	7.34	8.46	9.08		

Quantification: **D**: For each type of DHS in each sex, to calculate the depth of the K4me1 trough, the K4me1 read density at the DHS summit is subtracted from the K4me1 read density at the K4me1 maximum (the position at which K4me1 forms local maxima where there are bimodal peaks). Where K4me1 forms a trough, this value is positive, and if K4me1 forms a single peak, this value is negative. Next, for male-biased DHSs, the K4me1 trough depth in female liver is subtracted from that in male liver, and vice versa for female-biased DHSs.

For male-biased DHS sites, this value is highest where there is male-enriched FOXA1 binding or male-enriched FOXA2 binding (**bold, green**) and lowest where there is no FOXA1 or FOXA2 binding (**bold, red**) , and similarly for female-biased DHS sites , though to a much smaller degree. STAT5 binding does not confer as much difference as FOXA1 and FOXA2 do.

E: For each of (FOXA1-male, FOXA2-male, STAT5-male and CUX2) at male-biased DHSs, the difference in K4me1 profile between male and female liver is compared with and without binding of a second factor. For STAT5, the K4me1 profile difference is greatly intensified when it binds along with FOXA1/2 or CUX2.

Supp Figure S10 F-H Legend and conclusions

A Wilcoxon signed rank test was used to compare the DHS sex ratio and DHS read intensity in male between male-biased DHS that bind FOXA1/FOXA2 in a male-enriched or sex-independent manner from those that do not bind FOXA1/FOXA2. In **F**, Boxplots for p-values for FOXA1 and FOXA2 are shown in the table at the top. These results show that DHS where FOXA1/FOXA2 bind are more intense than those where they do not bind, and DHS where FOXA1/FOXA2 bind in a male-enriched manner are more sex-biased than those where they do not bind. This is what we would expect if FOXA1 and FOXA2 have chromatin opening activity.

In order to determine whether the deep trough in the K4me1 profile in male liver is related to FOXA1/FOXA2 binding, rather than just a feature of highly DNase hypersensitive sites or DHS with high male/female ratio in hypersensitivity regardless of FOXA1/FOXA2, samples were chosen from the non-FOXA binding set that matched the distributions in DHS intensity or DHS male/female ratio exhibited by the FOXA binding sets.

For each FOXA1/FOXA2 binding set, a matched non-FOXA binding set was chosen from male-biased DHS that bind neither FOXA1 nor FOXA2, either sex-independently or in a male-enriched manner. P-values of significance for difference between each FOXA binding set and its matched non-FOXA binding set are shown in the table at the bottom of Fig. **F**.

Figures G and H show K4me1 profiles at FOXA1-male-enriched binding sites, FOXA1-sex-independnt binding sites, FOXA2-male-enriched binding sites, and FOXA2-sex-independent binding sites, each compared to a matched background set of non-FOXA binding sites. The background sets were matched by either (**G**) DHS intensity in male or (**H**) DHS sex ratio. These figures support the conclusions from Fig. 7: **1)** sites with male-enriched FOXA1/FOXA2 have a deeper trough in K4me1 in male liver compared to those that lack FOXA binding, and **2)** sites with sex-independent FOXA1/FOXA2 binding have a bimodal K4me1 peak in both male liver and female liver, while those that lack FOXA binding have a monomodal K4me1 peak in female liver.

Supp Figure S10 F

F

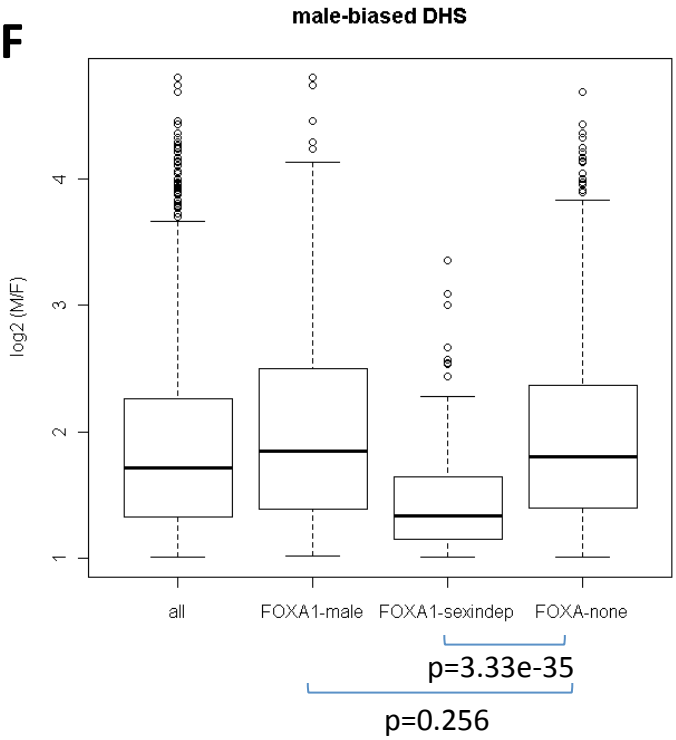

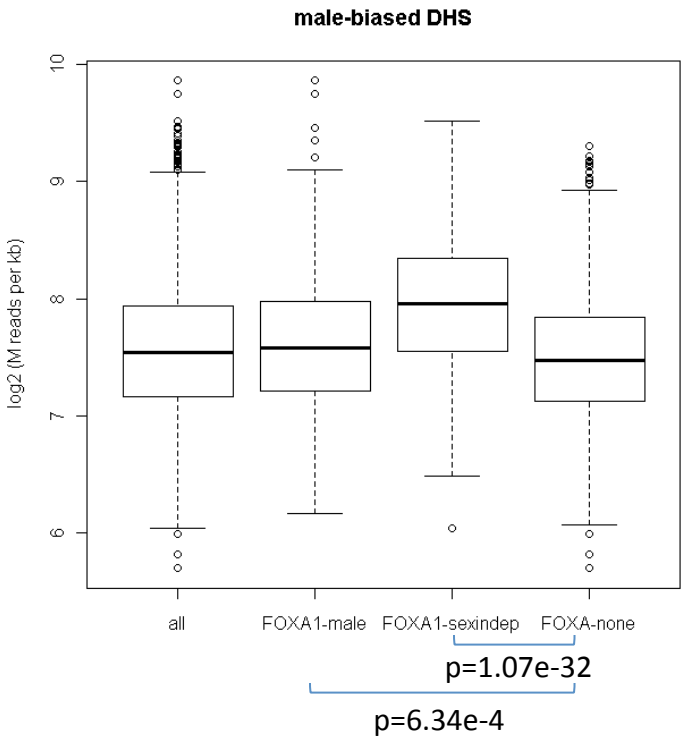

Background: all male-biased DHS that bind neither FOXA1 nor FOXA2	p-value for difference in distribution of DHS intensity or DHS sex ratio	
	DHS intensity	DHS sex ratio
FOXA1-male	6.34e-4	0.256
FOXA1-sexindep	1.07e-32	3.33e-35
FOXA2-male	0.964	2.04e-11
FOXA2-sexindep	4.34e-27	5.43e-54

Background: subset of male-biased DHS without FOXA binding that are matched by DHS intensity or DHS sex ratio to each foreground set	p-value for difference in distribution of DHS intensity or DHS sex ratio			
	Matched by DHS intensity		Matched by DHS M/F ratio	
	DHS intensity	DHS M/F ratio	DHS intensity	DHS M/F ratio
FOXA1-male	0.649	0.054	0.096	0.686
FOXA1-sexindep	0.350	7.24e-13	1.72e-11	0.812
FOXA2-male	0.827	5.24e-8	0.277	0.754
FOXA2-sexindep	0.364	6.72e-23	5.07e-9	0.754

Supp Figure S10 G

G

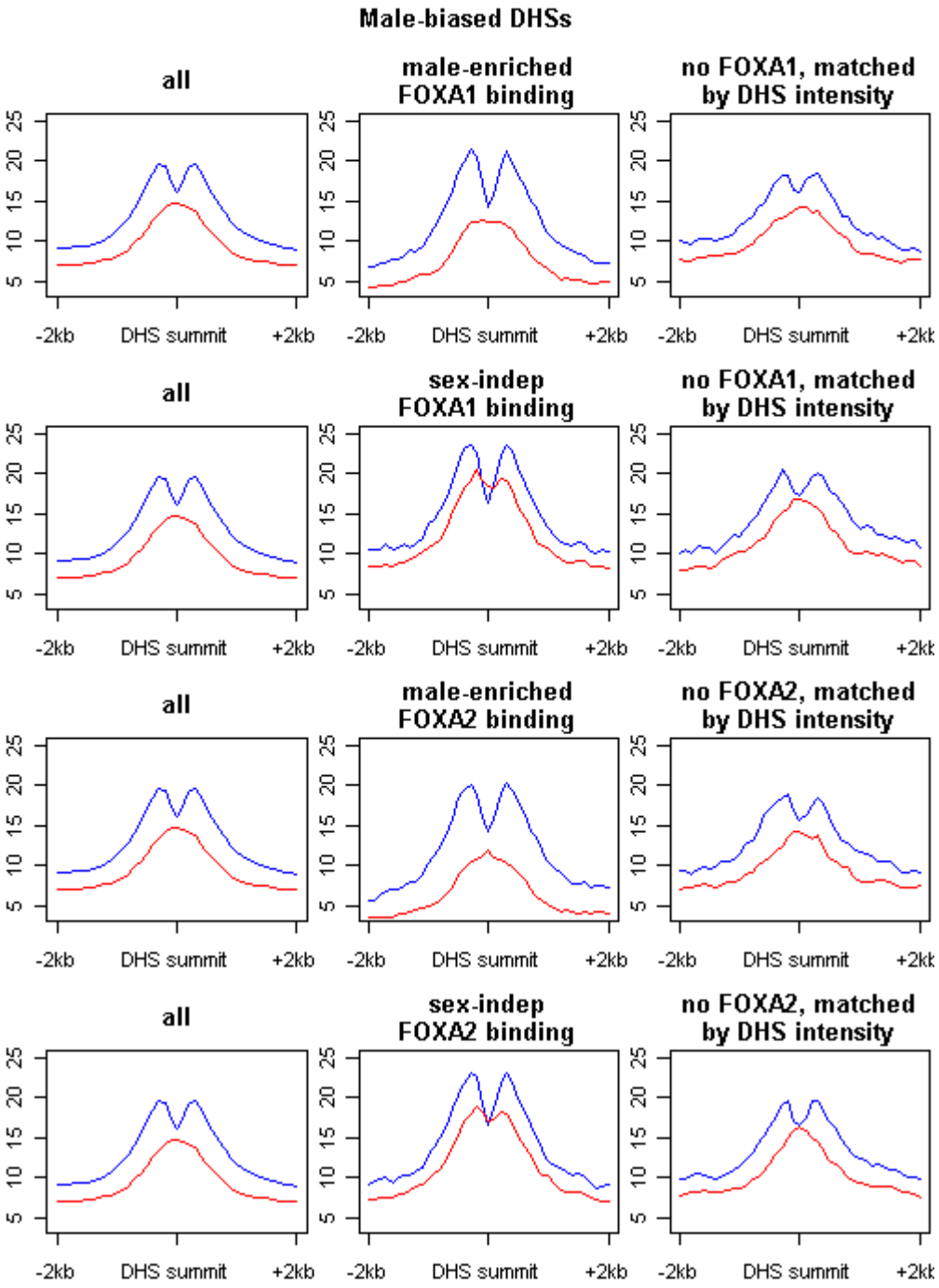

Supp Figure S10 H

H

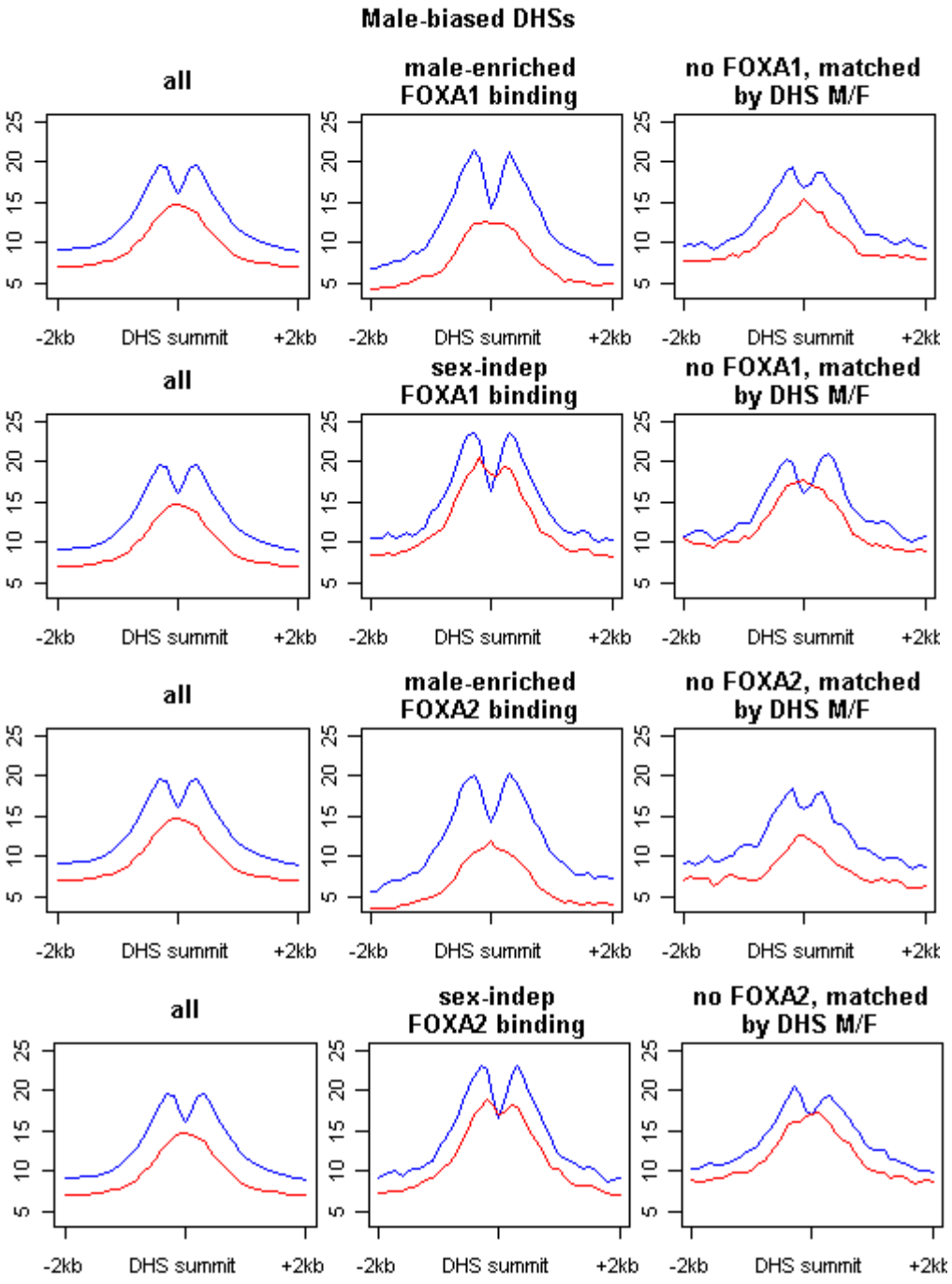

Supp Figure S11: UCSC Genome browser visualizations of chromatin marks at select genes.

The UCSC genome browser screenshots in this figure, on the following 6 pages, show the following genes, in order.

For chromatin marks, "M" indicates the gene has a male-enriched mark in the promoter (K4me3) or coding region (other modifications), "F" indicates a female-enriched mark, "I" indicates a sex-independent mark, and "N" indicates no mark in the promoter (K4me3) or coding region (other modifications).

	Gene	Class	RNA-seq M/F	K9me3	K27me3	K4me1	K27ac	K4me3	K36me3
A	***Cyp2b9* and *Cyp2b13***	Female F3 (both genes)	0.0068, 0.0166	N N	M M	F F	F F	N N	F F
B	***Elovl3***	Male M3	57.5	N	I	I	M	M	M
C	***Hsd3b5***	Male M4	7.53	N	N	M	M	M	M
D	***Sult2a6***	Female F2	0.0053	N	M	F	N	N	N
E	***Foxa1***	Male M1	1.52	N	N	I	I	I	I
F	***Cabyr***	Male M1	31.3	N	N	I	I	N	I

Fig. S11A - *Cyp2b13, Cyp2b9*

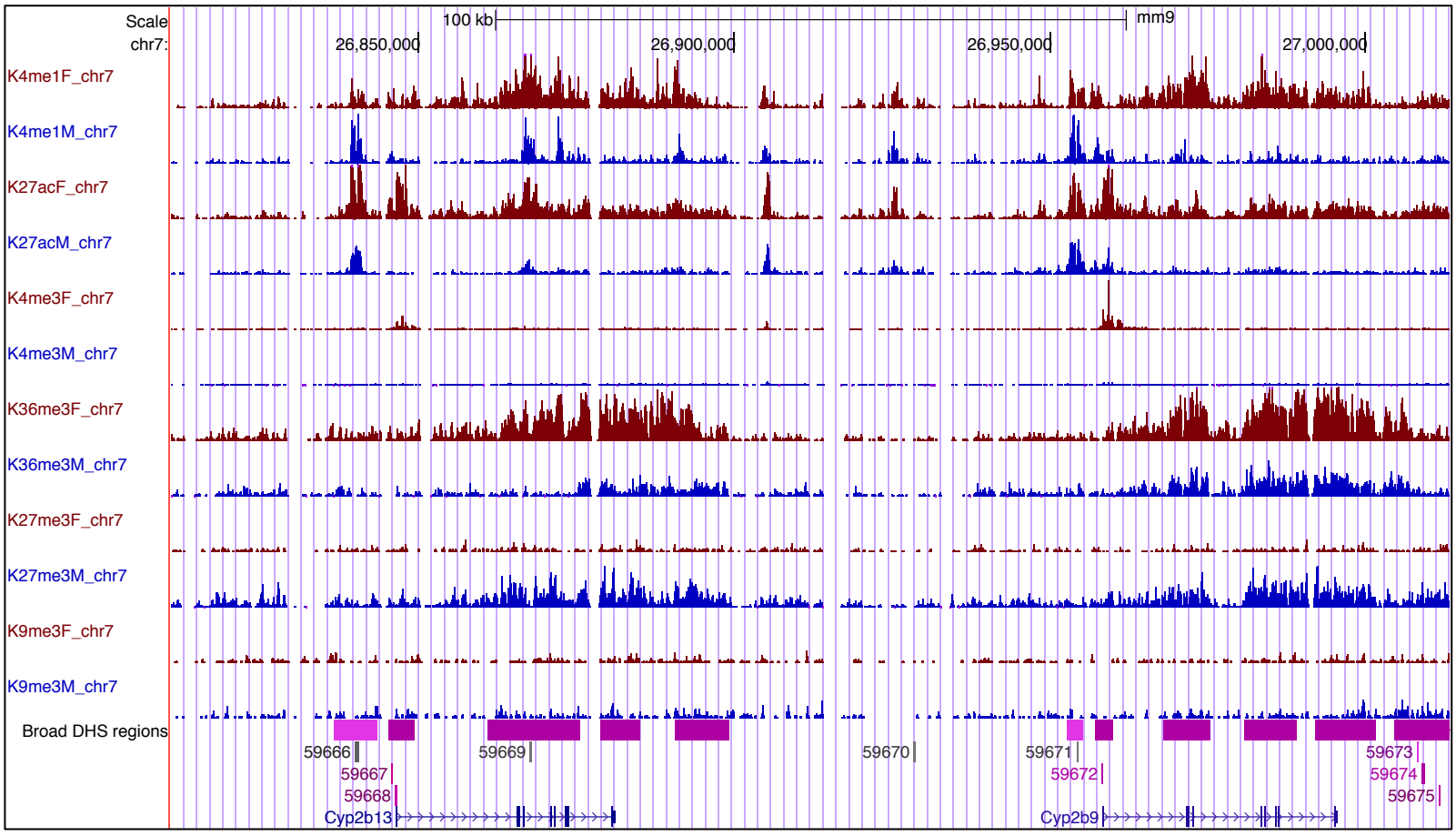

Fig. S11B – *Elovl3*

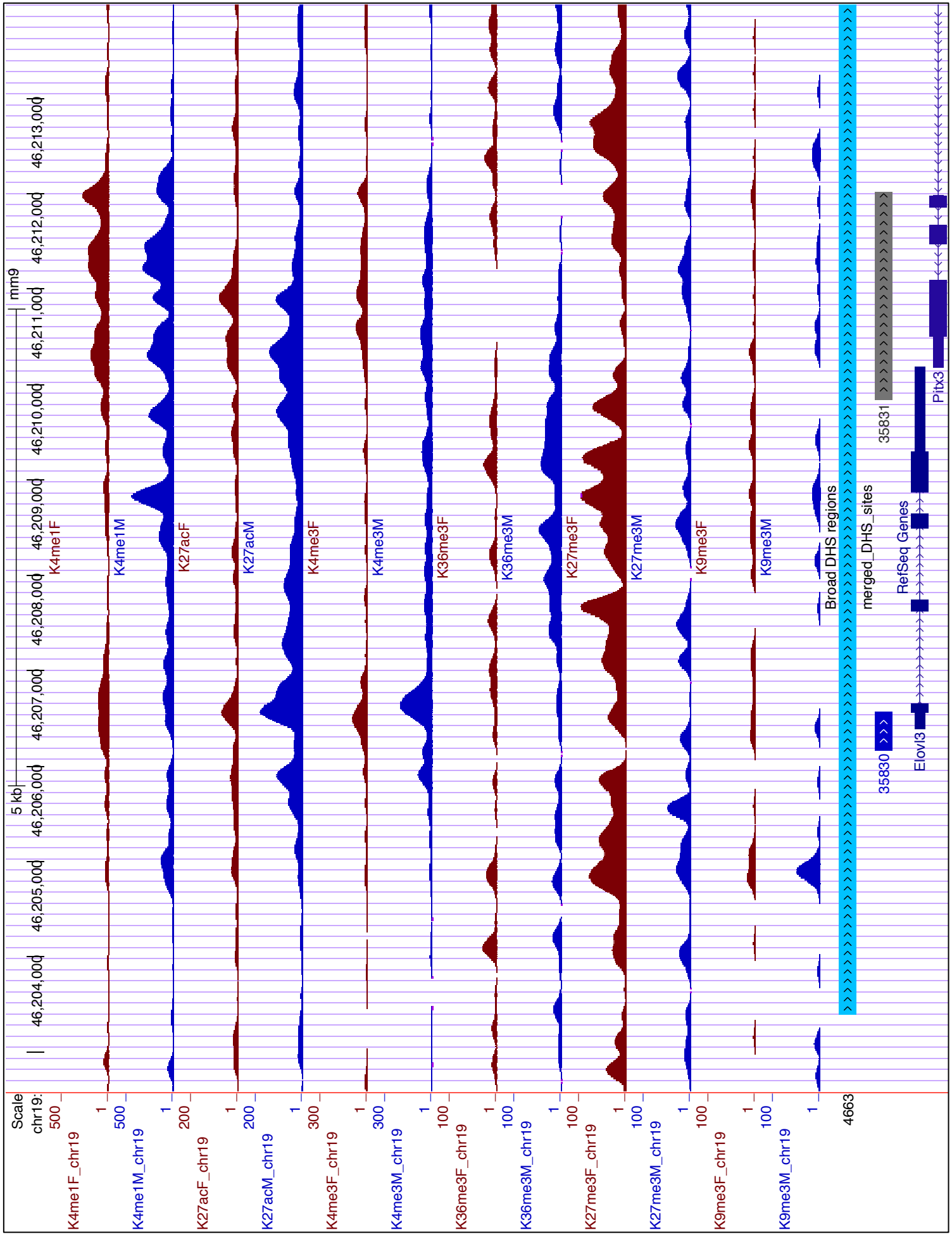

Fig. S11C
Hsd3b5

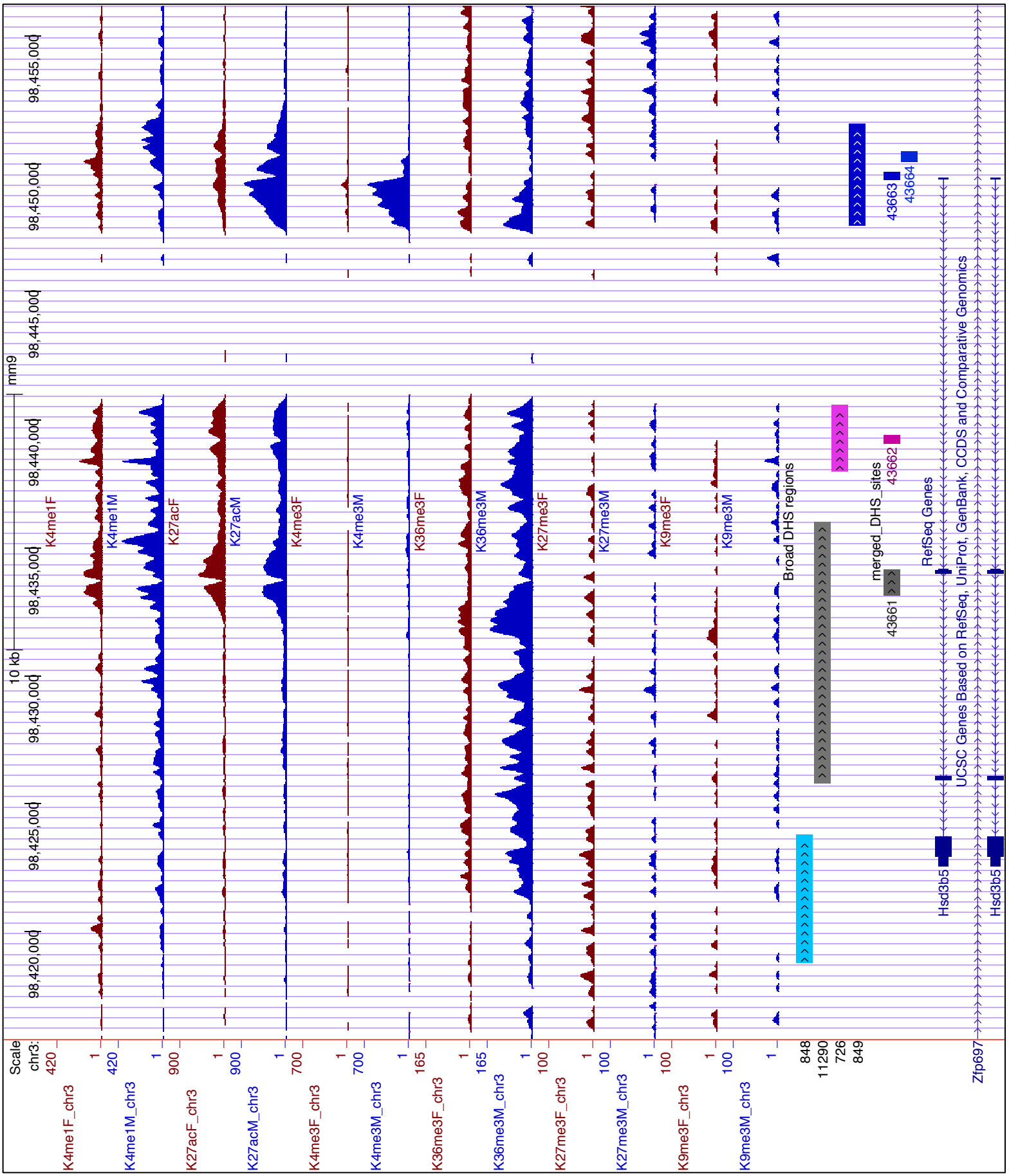

Fig. S11D - *Sult2a6*

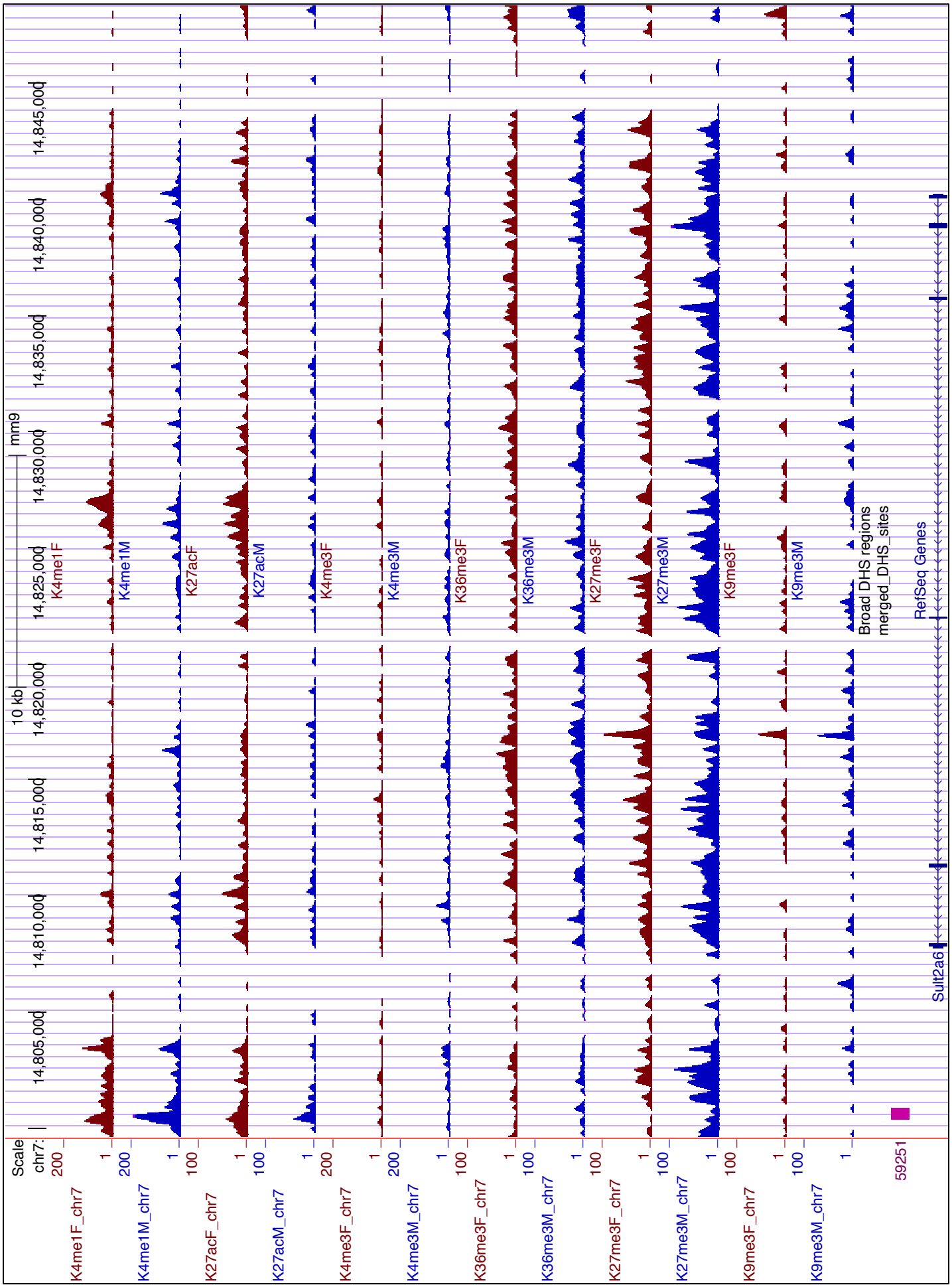

Fig. S11E – *Foxa1*

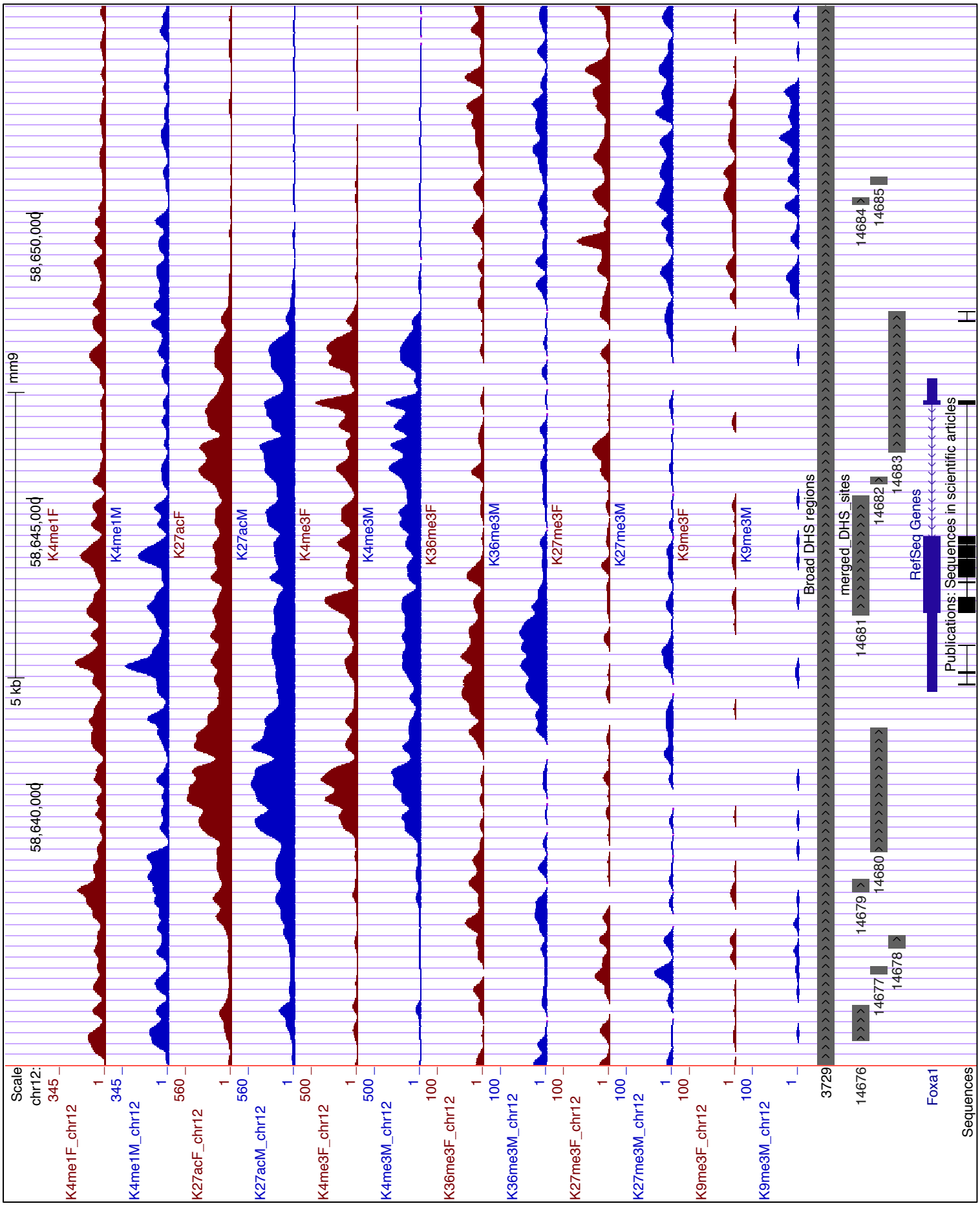

Fig. S11F
Cabyr

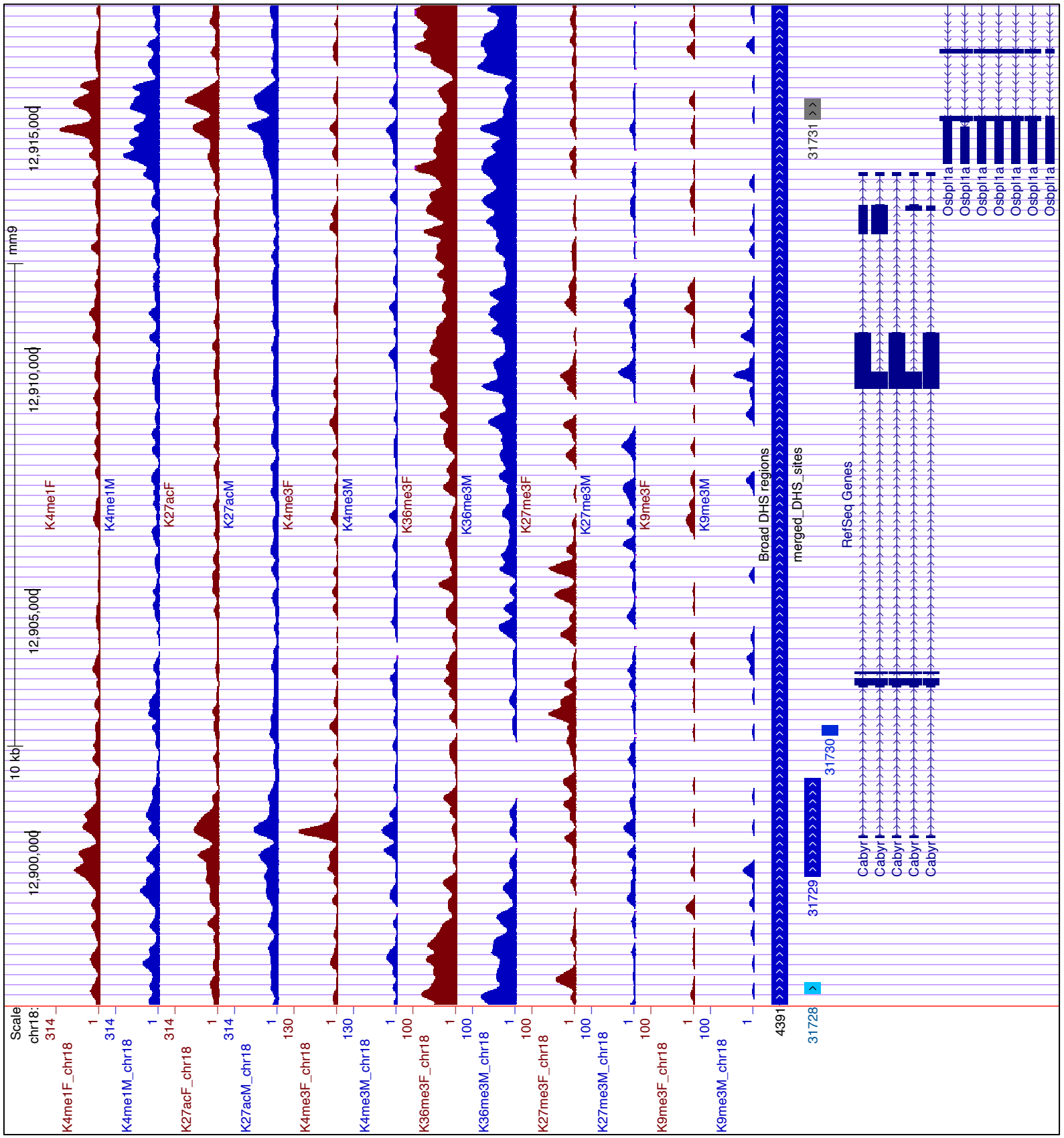

Supp figure S12: Choice of gap sizes for SICER. Shown are increasing total score of significant islands with increasing gap size. The gap size at which aggregate score plateaus was chosen. The second set of graphs show the same data as the first set of graphs, zoomed in on the y-axis. Left: male liver; right: female liver.

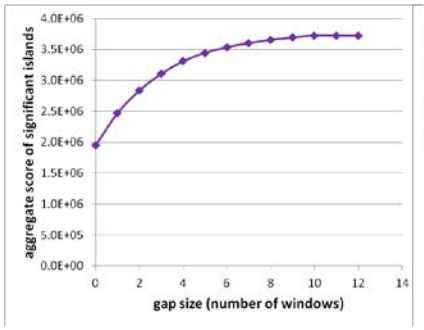

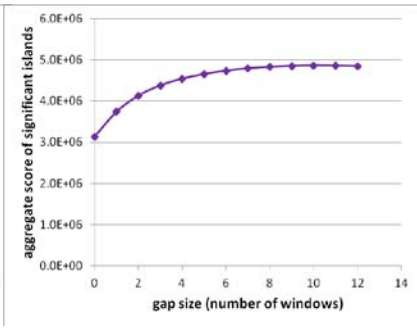

A: K27me3. Window size = 400 bp, and we chose gap size = 6 x window size = 2,400 bp.

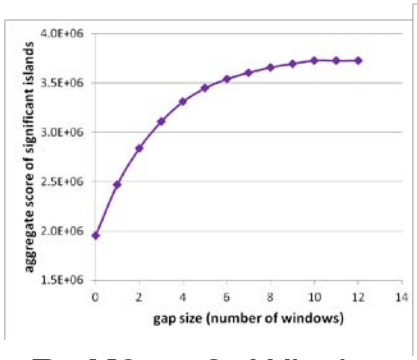

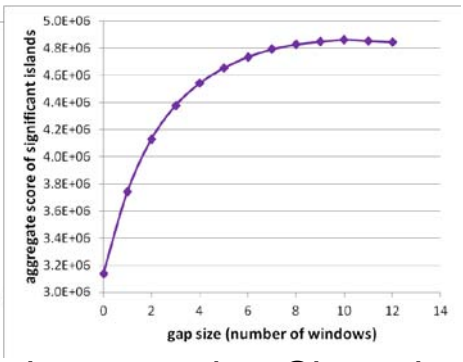

B: K9me3. Window size = 400 bp. Since there was no clear saturation point for male liver, we chose the same parameters as for K27me3.

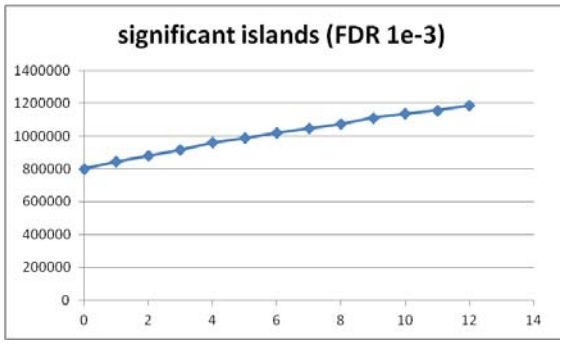

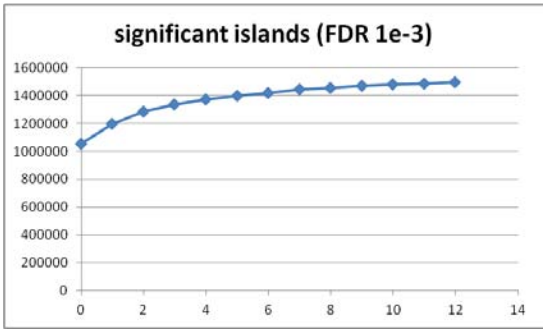

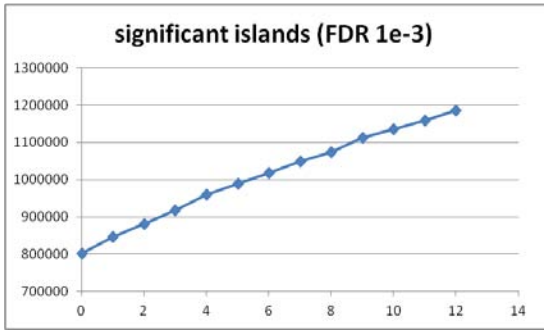

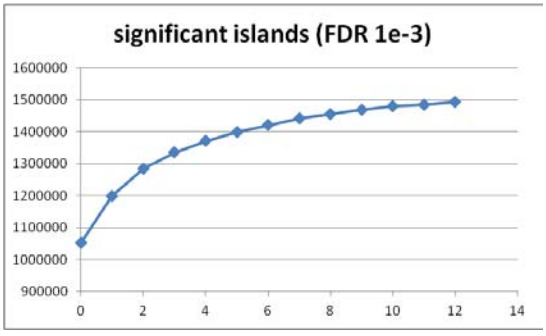

Supp Figure S12, continued: Choice of gap sizes for SICER. Shown are increasing total score of significant islands with increasing gap size. The gap size at which aggregate score levels off was chosen. The second set of graphs show the same data as the first set of graphs, zoomed in on the y-axis. Left: male liver; right: female liver.

C: K36me3. Window size = 200 bp. We chose gap size = 4 x window size = 800 bp.

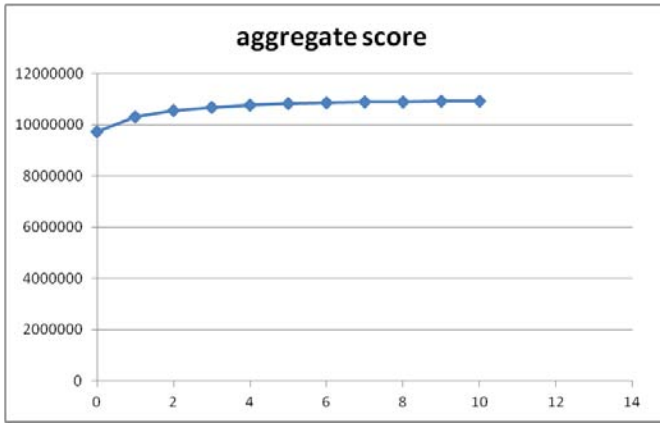

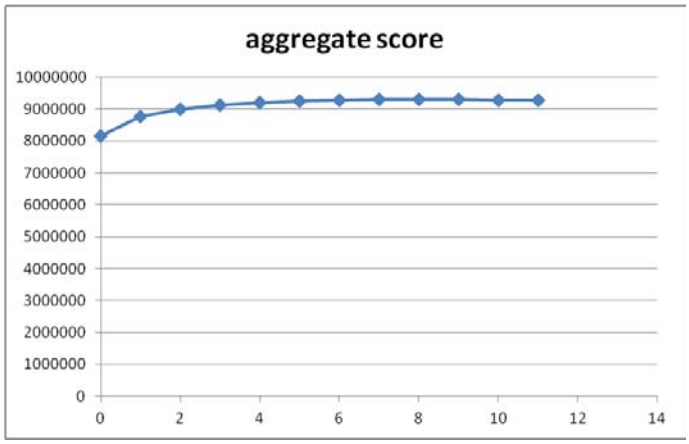

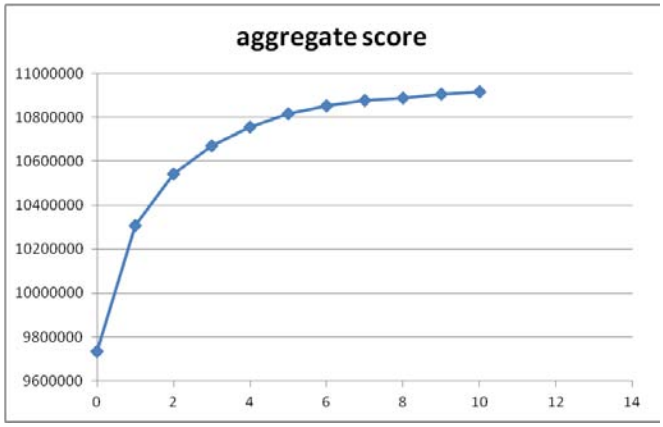

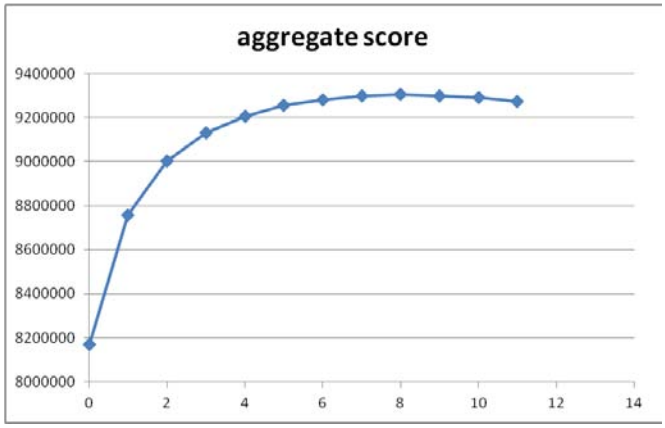

Supp Table S1. Lists of genes and DHS sites with associated chromatin marks and other characteristics. See additional Excel file.

A. All 15,533 genes clustered by chromatin mark read densities around TSS and TES (Fig. 3). For each gene, the cluster it belonged to in male liver and female liver are listed, along with RNA-seq data for liver expression, and whether or not it was regulated by one of the ligand-activated receptors (Fig. 3C-D)

B. Female-biased genes classified as shown in Table S4A. Columns D to AE indicate whether each gene had an associated chromatin modification, as shown in Fig. 4A and Fig. S6E. Columns AF to AJ indicate whether each gene had a TF binding site within 10kb, for which enrichments are shown in Fig. 5A.

C. Male-biased genes classified as shown in Table S4A. Columns D to AE indicate whether each gene had an associated chromatin modification, as shown in Fig. 4A and Fig. S6E. Columns AF to AJ indicate whether each gene had a TF binding site within 10kb, for which enrichments are shown in Fig. 5B.

D. All female-biased DHS classified by K27ac/K4me1 status, along with nearest sex-biased gene within 250kb, and whether or not they contain TF binding sites and are GH-responsive, for which enrichments are shown in Fig. 6B and Supp. Table S6B. If no gene is assigned, the DHS did not have a sex-biased gene within 250kb.

E. All male-biased DHS classified by K27ac/K4me1 status, along with nearest sex-biased gene within 250kb, and whether or not they contain TF binding sites and are GH-responsive, for which enrichments are shown in Fig. 6B and Supp. Table S6C. If no gene is assigned, the DHS did not have a sex-biased gene within 250kb.

F-G. Sex-independent DHS in female liver (**F**) and male liver (**G**) whose nearest gene TSS within 250 kb was sex-biased in expression. Shown are K27ac and K4me1 status, associated sex-biased gene, and whether or not they contain TF binding sites are GH-responsive. Since enrichments were similar for sex-independent DHS in male liver and female liver, the largest number was chosen in for each row in Fig. 6B and Supp. Table S6D.

Supp Table S2. DAVID annotation clusters meeting enrichment score > 1.5, for each of the six clusters shown in Fig. 3. See additional Excel file.

For each annotation cluster, the number of genes, name of first term, p-value of first term, all terms in annotation cluster, and genes matching all terms are listed.

A. cluster 1: most active
B. cluster 2: active
C. cluster 3: active
D. cluster 4: poised
E. cluster 5: poised
F. cluster 6: inactive

Supp Table S3. Chromatin mark peaks (identified using MACS) and regions (identified using SICER) and sex-bias.

A: Numbers of reads obtained and peaks/islands identified for each histone modification. K9me3, K27me3, and K36me3 marks were identified using SICER, and K4me1, K27ac, and K4me3 marks were identified using MACS. Sex-biased marks were identified by normalizing read counts by the M/F ratio in reads in common peaks, which accounts for differences between samples in % of reads in peaks.

Sex-biased marks were identified as those that had 2-fold higher reads in one sex than the other (|M|>1) and had p<0.001. Male-biased marks were obtained from lists of peaks/regions in male liver (Tables S3 B-G), and Female-biased marks were obtained from lists of peaks/regions in female liver (Tables S3 H-M). Choices of gap size for SICER are depicted in the Supp Figures S12.

Chromatin mark	Total reads (millions)		Peaks (MACS) or regions (SICER)					
	Male liver	Female liver	Total Peaks in Male liver	Total Peaks in Female liver	Male-biased (M>1 and p<0.001)	Female-biased (M<-1 and p<0.001)	Mean region length	Median region length
K9me3	10.7	14.6	10,875	17,626	372	394	14 kb	12 kb
K27me3	42.6	45.7	20,048	19,506	160	8	29 kb	22 kb
K4me1	39.3	52.5	74,275	82,944	6,098	3,219	2 kb	1.4 kb
K27ac	35.3	36.1	40,903	38,306	713	1,157	3 kb	2 kb
K4me3	41.2	36	16,018	18,942	714	237	2 kb	1.6 kb
K36me3	34.9	33.1	25,517	19,057	142	86	14 kb	9 kb

B-M: MACS or SICER data for each modification in livers of each sex, along with sex-specificity information. See additional Excel file.

- **B** K4me1 in male liver
- **C** K27ac in male liver
- **D** K4me3 in male liver
- **E** K9me3 in male liver
- **F** K27me3 in male liver
- **G** K36me3 in male liver
- **H** K4me1 in female liver
- **I** K27ac in female liver
- **J** K4me3 in female liver
- **K** K9me3 in female liver
- **L** K27me3 in female liver
- **M** K36me3 in female liver

Supp Table S4: Classes of sex-biased genes by chromatin cluster.

A. Each sex-biased gene was classified according to the cluster it belonged to in male liver and the cluster it belonged to in female liver (Fig. S6A). There are nine possible combinations for each set of sex-biased genes, which were collapsed into the six classes shown below (F1-F6 and M1-M6). A majority of sex-biased genes belonged to the same chromatin-based cluster in both male and female liver (classes F1, F2, and M1, M2), and were primarily associated with sex-independent chromatin marks (Fig. 4A and Fig. S6E). Although a small number of sex-biased genes (classes F5, F6 and M5, M6) apparently belong to a higher chromatin activity cluster in the sex where they are less highly expressed (e.g. F6 genes belong to the intermediate cluster among the three chromatin-based clusters of female-biased genes in female liver, but to the active chromatin cluster according to the independent clustering carried out for male liver) (Fig. 4A), a large majority of chromatin mark peaks and domains associated with these gene classes were either sex-independent or were absent, indicating that these genes do not exhibit significant sex-differences in chromatin that are opposite to the sex-difference in expression.

Female-biased genes				**Male-biased genes**			
Female liver	*Male liver*	*Gene count*	*Class*	*Male liver*	*Female liver*	*Gene count*	*Class*
Active	Active	100	F1	Active	Active	92	M1
Intermediate	Intermediate	184		Intermediate	Intermediate	175	
Inactive	Inactive	126	F2	Inactive	Inactive	100	M2
Active	Inactive	4	F3	Active	Inactive	4	M3
Intermediate	Inactive	17		Intermediate	Inactive	8	
Active	Intermediate	18	F4	Active	Intermediate	17	M4
Inactive	Active	0	F5	Inactive	Active	5	M5
Inactive	Intermediate	14		Inactive	Intermediate	3	
Intermediate	Active	14	F6	Intermediate	Active	19	M6

Supp Table S4 B-C: Enrichments for target genes of transcription factors STAT5, BCL6, CUX2, FOXA1 and FOXA2, along with p-values and numbers of genes. **B**: female-biased genes; **C**: male-biased genes. Fold-enrichment for being a target of each TF, compared to the background of all liver-expressed genes. Data is shown for enrichments that meet p<0.05 and that contain at least 5 genes. Numbers in parentheses next to each gene class indicate total number of genes in that class.

B

	STAT5-female			STAT5-sexindep			BCL6			CUX2			FOXA1-female			FOXA2-female			FOXA1-sexindep			FOXA2-sexindep		
	fold enrich	p-value	# genes	fold enrich	p-value	# genes	fold enrich	p-value	# genes	fold enrich	p-value	# genes	fold enrich	p-value	# genes	fold enrich	p-value	# genes	fold enrich	p-value	# genes	fold enrich	p-value	# genes
F1 (284)	2.83	1.3E-12	59	1.41	2.3E-06	136	1.64	4.8E-09	118	1.58	1.3E-02	31				3.35	8.0E-08	28				1.20	5.5E-04	180
F2 (126)	2.18	1.1E-03	21													3.91	9.8E-06	15	0.67	1.3E-06	54	0.83	4.8E-02	56
F3 (21)	6.20	1.2E-06	10							5.45	5.3E-05	8				7.63	4.1E-04	5						
F4 (18)	3.59	1.0E-02	5				1.94	2.8E-02	9															
F5 (14)	4.62	3.1E-03	5																					
F6 (14)				2.08	8.0E-03	10	3.05	5.5E-05	11															

C

	STAT5-male			STAT5-sexindep			BCL6			CUX2			FOXA1-male			FOXA2-male			FOXA1-sexindep			FOXA2-sexindep		
	fold enrich	p-value	# genes	fold enrich	p-value	# genes	fold enrich	p-value	# genes	fold enrich	p-value	# genes	fold enrich	p-value	# genes	fold enrich	p-value	# genes	fold enrich	p-value	# genes	fold enrich	p-value	# genes
M1 (267)	5.15	8.9E-31	75	1.78	9.7E-18	160	1.92	1.3E-15	129	2.50	3.2E-08	45	2.55	4.6E-12	65	4.27	5.1E-09	25	1.26	8.6E-09	214	1.45	1.0E-14	203
M2 (100)	2.65	3.6E-04	16	0.72	4.5E-02	25										2.53	3.4E-02	6						
M3 (12)													4.19	4.3E-03	5									
M4 (17)	6.78	3.6E-05	7	1.88	1.8E-02	11				9.32	1.7E-09	11	5.34	1.1E-05	9				1.38	4.2E-02	15			
M5 (8)																								
M6 (19)	4.31	4.9E-03	5	1.99	2.9E-03	13	2.04	1.5E-02	10		1.5E-01	3							1.40	2.8E-02	17	1.58	9.4E-03	16

Supp table S4D : Enrichment of sex-biased chromatin marks at female-biased genes (top) and male-biased genes (bottom) that are targets of TF binding. Enrichment = [(# genes with TFBS and chromatin mark)/(# genes with TFBS)] / [(# total genes with chromatin mark)/(total genes)]
Enrichments are shown if they meet Fisher Exact Test p-value <0.05 and contain at least 5 genes.

For each TF (columns) and each sex-biased chromatin modification (rows), the fold enrichment for co-occurrence at target female-biased genes *(top)* and male-biased genes *(bottom)*. Among female-biased genes (top), the highest fold enrichment is for CUX2 targets, having male-enriched K27me3.

D

Female-biased genes	CUX2	STAT5-female	BCL6	FOXA2-female
K9me3-male				
K27me3-male	4.69	2.75	1.39	4.30
K4me1-female	2.15	2.05	1.40	2.22
K27ac-female (gene body)	2.67	2.37	1.32	3.00
K27ac-female (promoter)	3.25	2.32		3.12
K4me3-female	3.47	2.55		2.81
K36me3-female	4.34	3.38		3.96

Male-biased genes	CUX2	STAT5-male	FOXA1-male	FOXA2-male
K9me3-female				
K27me3-female				
K4me1-male	1.67	1.77	1.67	1.74
K27ac-male (gene body)	1.63	1.89	2.07	4.02
K27ac-male (promoter)			2.25	3.57
K4me3-male		1.66	2.09	2.86
K36me3-male	2.20			

Supp Table S4E : Jaccard matrices for TF targets and chromatin marks for female-biased genes. Each value is (# Female-biased genes that are a target of a particular TF within 10kb **AND** contain a particular chromatin modification at the promoter or gene body)/(# Female-biased genes that are a target of a particular TF within 10kb **OR** contain a particular chromatin modification at the promoter or gene body).

	Female-biased genes	all	F1	F2	F3	F4	F5	F6
CUX2 with…	K9me3-male	**0.033**	0.029	0.083	0.000	0.000	0.000	0.000
	K27me3-male	**0.278**	0.167	0.353	0.583	0.250	0.000	0.000
	K4me1-female	**0.188**	0.153	0.185	0.500	0.000	0.200	0.000
	K27ac-female (gene body)	**0.220**	0.145	0.238	0.533	0.200	0.333	0.000
	K27ac-female (promoter)	**0.129**	0.083	0.063	0.417	0.000	0.000	0.000
	K4me3-female	**0.119**	0.028	0.083	0.417	0.250	0.000	0.000
	K36me3-female	**0.191**	0.083	0.188	0.600	0.333	0.000	0.000
STAT5-female with…	K9me3-male	**0.028**	0.016	0.091	0.000	0.000	0.000	0.000
	K27me3-male	**0.186**	0.111	0.259	0.500	0.167	0.000	0.000
	K4me1-female	**0.274**	0.207	0.387	0.533	0.000	0.800	0.000
	K27ac-female (gene body)	**0.284**	0.253	0.276	0.471	0.143	0.400	0.250
	K27ac-female (promoter)	**0.104**	0.031	0.167	0.462	0.000	0.000	0.000
	K4me3-female	**0.098**	0.048	0.091	0.357	0.167	0.000	0.000
	K36me3-female	**0.173**	0.081	0.364	0.385	0.200	0.000	0.000
BCL6 with…	K9me3-male	**0.017**	0.017	0.040	0.000	0.000	0.000	0.000
	K27me3-male	**0.098**	0.049	0.200	0.429	0.100	0.000	0.000
	K4me1-female	**0.224**	0.206	0.250	0.294	0.200	0.429	0.167
	K27ac-female (gene body)	**0.176**	0.137	0.258	0.333	0.200	0.143	0.182
	K27ac-female (promoter)	**0.053**	0.024	0.111	0.286	0.000	0.000	0.000
	K4me3-female	**0.059**	0.033	0.040	0.385	0.100	0.000	0.000
	K36me3-female	**0.063**	0.033	0.103	0.308	0.111	0.000	0.000
FOXA2-female with…	K9me3-male	**0.035**	0.032	0.059	0.000	0.000	0.000	0.000
	K27me3-male	**0.239**	0.147	0.400	0.231	0.333	0.000	0.000
	K4me1-female	**0.184**	0.127	0.321	0.286	0.000	0.000	0.333
	K27ac-female (gene body)	**0.240**	0.236	0.292	0.250	0.250	0.000	0.000
	K27ac-female (promoter)	**0.119**	0.059	0.158	0.273	0.000	0.000	0.000
	K4me3-female	**0.092**	0.063	0.059	0.167	0.333	0.000	0.000
	K36me3-female	**0.167**	0.059	0.333	0.182	0.500	0.000	0.000

Table S5 – Sex-biased DHS categorized by enhancer status and associated sex-biased gene classes

A: Presence of male-biased, female-biased, or sex-independent K4me1 or K27ac sites and their enrichment compared to background, comprised of all sex-independent DHS that are distant from sex-biased genes. DHS regions were defined as peak summit + 500 bp in both directions, and at least 200 bp overlap with a K4me1 or a K27ac site. **B-D:** Proximity of categories of DHS sites to classes of genes. For each set of DHS sites (male-biased (**B**), female-biased (**C**), and sex-independent (**D**)), the nearest sex-biased gene TSS within 250kb was obtained. Shown here are the number of DHS sites of each category that are nearest a sex-biased gene of each class, with the enrichment for that association compared to the background set of all sex-biased genes and all female-biased, male-biased, or sex-independent DHS sites. Enrichments and depletions that meet $p<0.05$ are shown. Subsets of male-biased DHS sites are enriched at female-biased genes and may be silencers.

Table **A** shows that sex-biased DHS are enriched for the presence of sex-biased K27ac or K4me1 marks.

Tables **B** and **C** show that sex-biased gene classes F3 and M3, which comprise the most highly sex-biased genes, are enriched for association (within 250 kb) with sex-biased DHS that have sex-biased K27ac, the mark of an active enhancer. Similarly, among sex-independent DHS (Table **D**), the highest enrichments are for association between sites with sex-biased K27ac and F3 and M3 genes. For class F3 but not class M3 genes, the enrichment is independent of K4me1 status. Some male-biased DHS also show enrichment for association with female-biased genes (Table **C**); these may be repressive regulatory sites.

A	**Female-biased DHS**				**Male-biased DHS**			
			Enrichment				*Enrichment*	
Enhancer status	# sites	% of sites	*p-value*	*fold enrich*	# sites	% of sites	*p-value*	*fold enrich*
Female-enriched K4me1 and/or K27ac	460	35%	***0.0E+00***	***18.1***	5	0%	*1.3E-12*	*0.12*
Male-enriched K4me1 and/or K27ac	6	0%	*1.1E-04*	*0.26*	804	30%	***0.0E+00***	***16.3***
Sex-independent K4me1 and K27ac	453	34%	*1.2E-38*	*0.65*	1285	47%	*4.1E-03*	*0.94*
Sex-independent K4me1 only	304	23%	*4.6E-04*	*1.21*	221	8%	*6.8E-11*	*0.67*
Sex-independent K27ac only	7	1%	*9.2E-20*	*0.11*	140	5%	*2.6E-05*	*0.72*
Neither K4me1 nor K27ac	99	7%	*5.2E-40*	*0.36*	259	10%	*2.0E-103*	*0.36*

Supp table S5B-C: Proximity of categories of DHS sites to classes of genes.

For each set of DHS sites (male-biased (**B**), female-biased (**C**), and sex-independent (**D**)), the nearest sex-biased gene TSS within 250kb was obtained. Shown here are the number of DHS sites of each category that are nearest a sex-biased gene of each class, with the enrichment for that association compared to the background set of all sex-biased genes and all female-biased, male-biased, or sex-independent DHS sites. Enrichments and depletions that meet p<0.05 are shown. Subsets of male-biased DHS sites are enriched at female-biased genes and may be silencers.

B. Female-biased DHS sites

Enhancer status		Gene class for nearest sex-biased gene		# sites	fold enrichment	p-value
K4me1	K27ac					
female	female	female	F3	8	4.09	1.2E-03
female	female	female	F5	5	10.99	2.8E-04
female	female	female	F2	12	2.24	1.0E-02
female	sex-indep	female	F1	13	2.06	7.9E-03
sex-indep	female	female	F1	45	1.65	1.5E-03
sex-indep	female	female	F3	20	4.47	8.1E-07
sex-indep	female	female	F2	26	1.73	1.2E-02
none	female	female	F3	5	5.26	2.9E-03
none	female	female	F2	11	4.47	1.7E-05
sex-indep	sex-indep	female	F3	8	0.36	4.0E-03
sex-indep	sex-indep	female	F2	27	0.51	6.2E-04
sex-indep	none	female	F3	3	0.21	1.8E-03
none	none	female	F1	5	0.33	8.7E-04

C. Male-biased DHS sites

Enhancer status		Gene class for nearest sex-biased gene		# sites	fold enrichment	p-value
K4me1	K27ac					
male	male	male	M3	16	7.01	4.7E-08
male	male	female	F2	13	2.85	1.6E-03
sex-indep	sex-indep	male	M1	267	1.22	1.2E-02
sex-indep	sex-indep	male	M6	19	2.64	1.9E-02
sex-indep	sex-indep	male	M2	75	1.49	2.5E-02
sex-indep	sex-indep	female	F1	73	1.45	3.7E-02
sex-indep	none	female	F2	11	2.30	1.8E-02
none	sex-indep	male	M1	56	2.27	2.2E-09
none	sex-indep	male	M4	22	6.52	5.8E-11
male	none	male	M1	16	0.40	9.4E-06
male	none	female	F1	3	0.29	1.6E-02
sex-indep	sex-indep	male	M4	28	0.56	1.0E-02
sex-indep	sex-indep	male	M3	13	0.50	4.2E-02
sex-indep	none	male	M1	10	0.23	1.4E-10
sex-indep	none	male	M4	1	0.14	1.3E-02
sex-indep	none	male	M3	0	0.00	4.5E-02

Table S5D: Proximity of categories of DHS sites to classes of genes. Sex-independent DHS sites shown here are limited to those whose nearest gene is sex-biased.

Sex-independent DHS sites, female liver

Enhancer status		Gene class for nearest sex-biased gene		# sites	fold enrichment	p-value
K4me1	K27ac					
female	female	female	F1	19	1.54	2.3E-02
female	female	female	F3	8	18.30	1.4E-08
female	sex-indep	female	F4	7	6.93	6.4E-05
female	sex-indep	female	F2	9	2.30	1.4E-02
female	none	female	F1	61	1.56	4.6E-05
female	none	female	F5	6	2.46	3.8E-02
sex-indep	female	male	M6	15	1.98	1.4E-02
sex-indep	female	female	F1	95	1.45	2.6E-05
sex-indep	female	female	F4	26	5.51	7.5E-12
sex-indep	female	female	F3	21	9.88	4.3E-14
sex-indep	sex-indep	male	M1	2106	1.32	3.5E-21
sex-indep	sex-indep	male	M4	157	1.50	3.2E-03
sex-indep	male	male	M1	50	1.56	2.1E-04
sex-indep	male	male	M4	11	4.97	1.7E-05
sex-indep	male	male	M3	6	5.19	1.3E-03
sex-indep	none	female	F6	40	1.55	1.7E-02
sex-indep	none	female	F2	202	1.44	2.1E-06
male	sex-indep	male	M2	14	2.49	1.3E-03
male	male	male	M1	21	2.07	7.6E-05
male	male	male	M3	5	13.66	3.4E-05
male	none	male	M4	6	5.23	1.0E-03
none	female	female	F2	6	3.61	4.2E-03
none	sex-indep	male	M4	25	2.26	3.6E-04
none	sex-indep	male	M6	44	2.42	3.2E-07
none	sex-indep	male	M3	15	2.63	1.2E-03
none	male	male	M1	17	1.79	4.8E-03
none	none	male	M5	19	1.74	4.1E-02
none	none	female	F3	29	1.62	2.6E-02
none	none	female	F2	302	2.39	2.4E-36
female	female	male	M1	0	0.00	5.0E-07
female	sex-indep	male	M1	5	0.38	6.1E-03
female	none	male	M1	15	0.38	5.6E-07
female	none	male	M6	0	0.00	1.5E-02
sex-indep	female	male	M1	2	0.03	1.1E-31
sex-indep	female	male	M2	4	0.25	5.0E-04
sex-indep	sex-indep	male	M3	57	0.64	1.7E-02
sex-indep	sex-indep	female	F3	40	0.35	9.3E-09
sex-indep	sex-indep	female	F2	350	0.41	2.1E-47
sex-indep	male	female	F1	5	0.15	1.6E-11
sex-indep	male	female	F2	3	0.31	2.4E-02
sex-indep	none	male	M4	13	0.33	5.1E-06
sex-indep	none	male	M5	5	0.38	2.6E-02
sex-indep	none	female	F4	20	0.47	4.1E-04
male	male	female	F1	1	0.10	7.6E-05
male	none	female	F1	8	0.48	9.8E-03
none	female	male	M1	1	0.18	1.8E-02
none	female	female	F1	1	0.18	1.8E-02
none	sex-indep	male	M1	132	0.79	1.3E-03
none	male	female	F1	2	0.21	1.3E-03
none	none	male	M1	407	0.76	2.3E-10
none	none	male	M4	17	0.42	1.7E-04
none	none	male	M6	41	0.64	4.3E-03
none	none	female	F1	486	0.92	4.1E-02

Sex-independent DHS sites, male liver

Enhancer status		Gene class for nearest sex-biased gene		# sites	fold enrichment	p-value
K4me1	K27ac					
female	female	female	F1	20	1.81	3.1E-03
female	female	female	F3	6	19.33	7.8E-07
female	sex-indep	female	F4	6	7.44	1.5E-04
female	none	female	F1	40	1.39	1.8E-02
female	none	female	F2	25	2.90	9.7E-07
sex-indep	female	male	M6	16	2.20	3.6E-03
sex-indep	female	female	F1	96	1.69	2.9E-09
sex-indep	female	female	F4	18	4.61	1.6E-07
sex-indep	female	female	F3	17	11.80	7.8E-13
sex-indep	female	female	F2	28	1.63	1.0E-02
sex-indep	sex-indep	male	M1	2437	1.34	1.6E-28
sex-indep	sex-indep	female	F1	1972	1.08	4.7E-03
sex-indep	male	male	M1	65	1.48	1.5E-04
sex-indep	male	male	M4	10	2.39	1.0E-02
sex-indep	male	male	M2	18	1.71	2.3E-02
sex-indep	male	female	F5	6	2.58	3.1E-02
sex-indep	none	male	M2	113	1.30	7.5E-03
sex-indep	none	female	F6	33	1.84	2.3E-03
sex-indep	none	female	F2	136	1.43	7.7E-05
male	sex-indep	male	M1	68	1.28	1.7E-02
male	sex-indep	male	M4	15	2.99	2.0E-04
male	sex-indep	male	M2	28	2.20	9.0E-05
male	male	male	M3	7	9.20	1.2E-05
male	none	male	M4	9	3.63	8.9E-04
none	female	female	F4	8	7.40	1.3E-05
none	female	female	F3	6	13.90	5.7E-06
none	female	female	F2	12	2.60	1.7E-03
none	sex-indep	male	M4	84	2.97	4.3E-16
none	sex-indep	male	M6	55	1.46	1.0E-02
none	sex-indep	male	M3	26	1.79	1.0E-02
none	male	male	M1	12	1.72	3.1E-02
none	none	female	F2	397	2.46	3.7E-46
female	female	male	M1	0	0.00	3.6E-07
female	sex-indep	male	M1	6	0.46	1.5E-02
female	none	male	M1	15	0.45	4.9E-05
sex-indep	female	male	M1	3	0.05	1.8E-30
sex-indep	female	male	M4	1	0.16	2.3E-02
sex-indep	female	male	M2	2	0.13	2.4E-05
sex-indep	sex-indep	male	M3	73	0.58	2.5E-04
sex-indep	sex-indep	male	M2	469	0.80	4.5E-04
sex-indep	sex-indep	female	F3	34	0.41	9.5E-06
sex-indep	sex-indep	female	F5	94	0.66	2.7E-03
sex-indep	sex-indep	female	F2	348	0.41	1.6E-49
sex-indep	male	female	F1	10	0.26	6.5E-10
sex-indep	male	female	F2	4	0.34	1.3E-02
sex-indep	none	male	M1	296	0.78	3.7E-07
sex-indep	none	male	M4	15	0.40	7.1E-05
male	sex-indep	male	M6	0	0.00	3.1E-03
male	sex-indep	female	F1	24	0.51	2.0E-05
male	sex-indep	female	F2	7	0.49	4.8E-02
male	male	female	F1	2	0.13	3.9E-06
male	none	female	F1	8	0.34	7.3E-05
none	female	male	M1	0	0.00	5.1E-10
none	sex-indep	female	F1	250	0.81	1.1E-04
none	sex-indep	female	F3	3	0.31	3.4E-02
none	sex-indep	female	F2	69	0.74	9.6E-03
none	male	female	F1	1	0.16	1.3E-02
none	none	male	M1	649	0.80	4.9E-11
none	none	male	M4	39	0.46	5.3E-07
none	none	male	M6	64	0.67	2.0E-03

Supp Tables S6. **A**: categorization of DHS by enhancer modifications. **B-D:** Enrichment for STAT5, BCL6, CUX2, and FOXA1/2 binding at categories of (**B**) Female-biased DHS, (**C**) Male-biased DHS, and (**D**) Sex-independent DHS.

A. Categories of DHS by enhancer-associated modifications.

Category	K27ac mark at DHS	K4me1 mark at DHS
K27ac_female	Female-biased	Any
K4me1_female	Sex-independent or absent	Female-biased
K27ac_male	Male-biased	Any
K4me1_male	Sex-independent or absent	Male-biased
K27ac_sex-indep	Sex-independent	Sex-independent or absent
K4me1_sex-indep	Absent	Sex-independent
neither	Absent	Absent

B-D. (See additional Excel file) show enrichments for TF binding at categories of male-biased (**B**), female-biased (**C**), and sex-independent (**D**) DHS, shown in Figure 6B, and also for subsets of each category of DHS that map to different classes of sex-biased genes. In tables **B-D**, columns that had no enrichments or depletions ($p<0.001$, and at least 5 sites for enrichment) are not shown.

To obtain target genes, each DHS was mapped to the nearest gene TSS within 250 kb, allowing for the possibility of distal regulation; specifically, the nearest sex-biased gene TSS for sex-biased DHS, and the nearest liver-expressed gene TSS for sex-independent DHS. The 250 kb limit was chosen based on the observation made using 5C technology (Sanyal et al., 2012) that most long-range interactions occur within 250 kb of the TSS, and the frequency of interactions peaks ~120 kb upstream of the TSS. Enrichments for TF binding were calculated for each category of sex-biased DHS, and for sex-independent DHS whose nearest gene TSS was sex-biased in its expression. Tables S6 **B-D** also show the numbers of DHS in each enriched or depleted group and their associated p-value.

Supp Tables S7. Evaluation of data quality for histone modification ChIP-seq samples. Tables S7 A-G are shown in the following pages.

List of samples is below. Two K27me3 samples were excluded due to high % reads in straight peaks (5% to 12%) and low peak overlap with the other replicates. One K4me1 and one K4me3 sample were both excluded due to low peak overlap with the other replicates, low read count correlation with the other replicates, and low overlap with DHS peaks and Robertson et al (2008) K4me1 and K4me3 peaks. Raw sequence reads for all of the following samples are available at the Gene Expression Omnibus (GEO) website as series **GSE44571** (samples GSM1087069-GSM1087105).

K4me1M: G68-M2, G75-M1, G75-M2, G75-M3
K4me1F: G68-M3, G72-M2, G75-M7a
K4me3M: G69-M2, G75-M4, G75-M5a, G75-M6a
K4me3F: G69-M3, G69-M4, G75-M8a
K36me3M: G76-M5a, G78-M3
K36me3F: G76-M6a, G78-M4
K27acM: G76-M1a, G76-M2a, G78-M1
K27acF: G76-M3a, G76-M4a, G78-M2
K27me3M: G43, G64-M1, G64-M2
K27me3F: G44, G67-M1, G67-M2
K9me3M: G63-M2, G67-M4
K9me3F: G63-M1, G67-M3

A. Numbers of reads in each sample and percentage of reads in each sample that were in straight peaks (>= 5 identical reads with no overlapping reads)

B-G: Concordance between replicates for each of the six chromatin modifications.

Table S7A

_2 indicates the same sample sequenced a second time to obtain additional data.

sample	sample ID	total mapped reads	sex	% reads in straight peaks (>5 identical reads with no overlapping reads)	Mouse ID
K27me3	G43_1	13,572,567	M	0.14%	229A3/A4
	G43_2	12,322,515	M	0.16%	229A3/A4
	G44_1	11,986,335	F	0.31%	229B1
	G44_2	14,081,981	F	0.85%	229B1
	G64-M1	8,367,220	M	0.00%	229A8-9
	G64-M2	8,709,625	M	0.00%	229A2
	G67-M1	4,992,142	F	0.00%	244B1
	G67-M1_2	6,152,424	F	0.00%	244B1
	G67-M2	4,193,312	F	0.01%	229B2
	G67-M2_2	4,728,768	F	0.02%	229B2
K9me3	G63-M2	5,628,066	M	0.13%	229A1
	G67-M4	3,005,383	M	0.00%	229A8
	G67-M4_2	2,828,892	M	0.00%	229A8
	G63-M1	7,896,586	F	0.00%	229B2
	G67-M3	3,398,248	F	0.00%	244B1
	G67-M3_2	3,632,324	F	0.00%	244B1
K4me1	G68-M2	5,936,415	M	0.00%	229A1
	G68-M2_2	8,662,540	M	0.00%	229A1
	G75-M1	7,996,457	M	0.27%	263A4
	G75-M2	8,425,897	M	0.18%	263A6
	G75-M3	8,343,902	M	0.22%	263A5
	G68-M3	7,807,478	F	0.00%	244B1
	G68-M3_2	12,541,970	F	0.00%	244B1
	G72-M2	6,459,972	F	0.00%	229B2
	G72-M2_2	11,185,147	F	0.01%	229B2
	G75-M7a	14,564,434	F	0.26%	263B5
K4me3	G69-M2	4,364,291	M	0.00%	229A1
	G69-M2_2	5,245,080	M	0.00%	229A1
	G75-M4	8,063,927	M	0.52%	263A4
	G75-M5a	7,654,489	M	0.84%	263A6
	G75-M6a	10,210,133	M	1.20%	263A5
	G69-M3	4,451,323	F	0.00%	244B1
	G69-M3_2	4,884,084	F	0.00%	244B1
	G69-M4	4,295,146	F	0.00%	229B2
	G69-M4_2	4,439,191	F	0.00%	229B2
	G75-M8a	8,134,883	F	0.90%	263B5
K36me3	G76-M5a	15,271,012	M	0.40%	263A6
	G78-M3	20,063,141	M	0.00%	263A5
	G76-M6a	17,819,539	F	0.42%	263B5
	G78-M4	15,741,169	F	0.00%	263B3
K27ac	G76-M1a	13,298,229	M	0.16%	263A6
	G76-M2a	11,503,440	M	0.19%	263A5
	G78-M1	16,479,192	M	0.16%	263A12
	G76-M3a	11,972,778	F	0.16%	263B5
	G76-M4a	11,128,093	F	0.19%	263B3
	G78-M2	12,974,469	F	0.14%	263B4

Supp Table S7B: Concordance between K27me3 replicates.

Percentage of peaks in each row sample that overlap a peak in each column sample in male liver (top) and female liver (bottom). Two samples were excluded due to high % reads in peaks (5% to 12%) and low peak overlap with other replicates (lowest overlaps 22% and 32%).

			Male liver		
			G43C	G64-M1	G64-M2
		# islands	7750	9228	8252
Male liver	G43C	7750		59%	63%
	G64-M1	9228	48%		40%
	G64-M2	8252	72%	57%	

			Female liver		
			G44C	G67-M1	G67-M2
		# islands	20069	14322	6837
Female liver	G44C	20069		45%	32%
	G67-M1	14322	82%		49%
	G67-M2	6837	91%	80%	

Supp Table S7-C: Concordance between K9me3 replicates

Percentage of islands in each row that overlap an island in each column

K9me3		# islands	male		
			G63M2	G67M4C	all male
male	G63M2	9565		30%	56%
	G67M4C	18142	17%		47%
	all male	10875	45%	70%	

K9me3		# islands	female		
			G63M1	G67M3C	all female
female	G63M1	10471		27%	51%
	G67M3C	11677	26%		73%
	all female	17626	28%	43%	

Correlation between reads in peaks:

K9me3		male	
		G63M2	G67M4C
male	G63M2		0.88
	G67M4C	0.88	

K9me3		female	
		G63M1	G67M3C
female	G63M1		0.82
	G67M3C	0.82	

Supp Table S7-D: Concordance between K36me3 replicates

Fraction of base pairs in peak regions in each row sample that overlap a peak region in each column sample.

K36me3		# bp in islands	male		
			G76M5	G78M3	all M
male	G76M5	284,813,400		0.85	0.93
	G78M3	277,764,800	0.87		0.96
	all M	308,875,600	0.86	0.87	

K36me3		# bp in islands	female		
			G76M6	G78M4	all F
female	G76M6	245,068,200		0.89	0.98
	G78M4	272,862,000	0.80		0.97
	all F	316,632,600	0.76	0.83	

Correlation between reads in peaks

K36me3		male	
		G76M5	G78M3
male	G76M5		0.96
	G78M3	0.96	

K36me3		female	
		G76M6	G78M4
female	G76M6		1.00
	G78M4	1.00	

The lowest correlation is 0.96 and the lowest overlap is 87%.

Supp Table S7E: Concordance between K27ac replicates. The lowest correlation is 0.96, the lowest overlap is 78%, and there are no outlier samples.

Fraction of peaks in each row sample that overlap a peak in each column sample.

K27ac		# peaks	male			
			G76M1	G76M2	G78M1	all M
male	G76M1	47059		0.78	0.80	0.92
	G76M2	43903	0.78		0.80	0.92
	G78M1	43610	0.77	0.76		0.93
	all M	40903	0.79	0.80	0.82	

K27ac		# peaks	female			
			G76M3	G76M4	G78M2	all F
female	G76M3	44145		0.74	0.80	0.92
	G76M4	40070	0.81		0.84	0.94
	G78M2	43024	0.75	0.72		0.91
	all F	38306	0.77	0.72	0.82	

Fraction of base pairs in peak regions in each row sample that overlap a peak region in each column sample.

K27ac		# bp	male			
			G76M1	G76M2	G78M1	all M
male	G76M1	86,870,761		0.82	0.85	0.97
	G76M2	89,112,933	0.80		0.84	0.96
	G78M1	95,888,524	0.77	0.78		0.97
	all M	124,526,423	0.67	0.69	0.74	

K27ac		# bp	female			
			G76M3	G76M4	G78M2	all F
female	G76M3	75,552,621		0.77	0.82	0.95
	G76M4	71,256,843	0.82		0.85	0.96
	G78M2	81,961,381	0.76	0.74		0.95
	all F	110,063,738	0.65	0.62	0.71	

Correlation between reads in peaks

K27ac		male		
		G76M1	G76M2	G78M1
male	G76M1		0.96	0.97
	G76M2	0.96		0.96
	G78M1	0.97	0.96	

K27ac		female		
		G76M3	G76M4	G78M2
female	G76M3		0.98	0.98
	G76M4	0.98		0.98
	G78M2	0.98	0.98	

Supp Table S7-F: Concordance between K4me1 replicates, and overlap with DHS sites (Ling et al., 2010) and with K4me1 peaks from Robertson et al., 2008. G68-M1 has consistently low overlap in both directions. i.e., a small fraction of G68-M1 peaks overlap with peaks from the other replicates (across) and a small fraction of peaks in other replicates overlap with G68-M1 peaks (down).

Bar charts show overlap with DNase hypersensitivity sites and literature K4me1 sites (Robertson et al., 2008) . The fraction of peaks that are within 150 bp of ~73,000 standard DHS sites, ~110,000 total DHS sites, and of K4me1 sites in female liver from Robertson et al.

One male sample was excluded due to low peak overlap with other replicates (lowest overlap 25% and lowest correlation 0.54) and low overlap with standard DHS (38%), all DHS (44%), and Robertson et al K4me1 peaks (72%).

Fraction of peaks in column sample that were found in row sample

K4me1 male	total peaks	G68_M2	G75_M1	G75_M2	G75_M3	All males
G68_M2	85666		31%	36%	34%	86%
G75_M1	40839	69%		72%	69%	95%
G75_M2	48047	69%	59%		65%	94%
G75_M3	43948	71%	62%	70%		95%
All males	71820	79%	36%	43%	40%	

correlation between reads in peaks

K4me1M	G68_M2	G75_M1	G75_M2	G75_M3
G68_M2		0.90	0.71	0.84
G75_M1	0.90		0.88	0.97
G75_M2	0.71	0.88		0.94
G75_M3	0.84	0.97	0.94	

Fraction of peaks in column sample that were found in row sample

K4me1 female	total peaks	G68_M3	G72_M2	G75_M7a	All females
G68_M3	92324		75%	61%	95%
G72_M2	83637	79%		60%	93%
G75_M7a	58282	82%	77%		93%
All females	76583	78%	73%	57%	

correlation between reads in peaks

K4me1F	G68_M3	G72_M2	G75_M7
G68_M3		0.95	0.87
G72_M2	0.95		0.83
G75_M7	0.87	0.83	

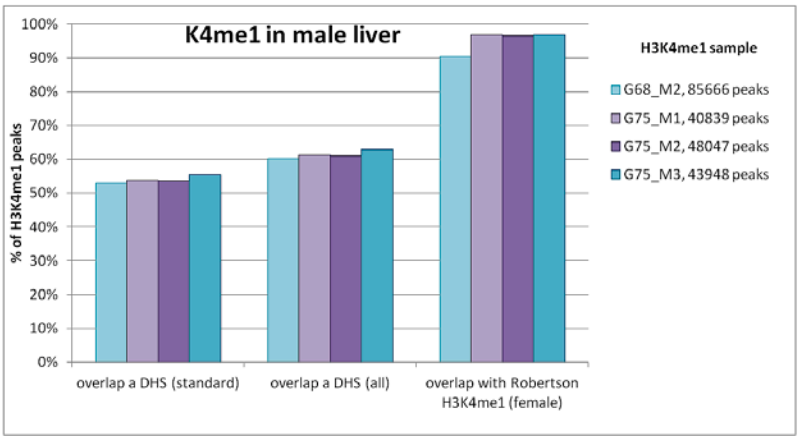

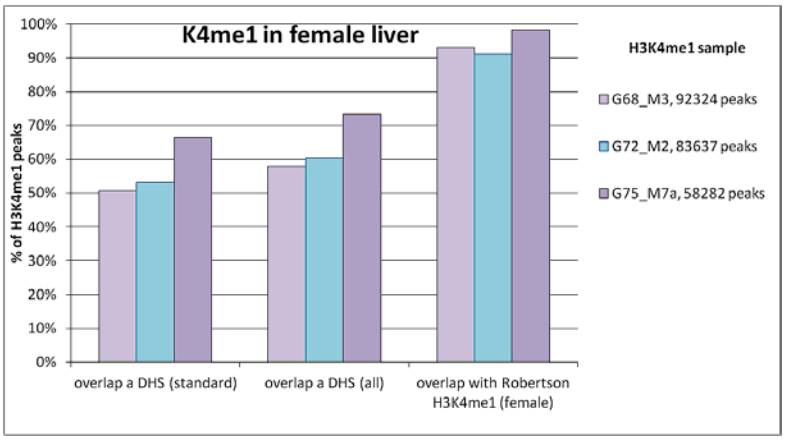

Supp Table S7-G: Concordance between K4me3 replicates, and overlap with DHS sites (Ling et al., 2010) and with K4me3 peaks from Robertson et al., 2008.

G69-M1 has consistently low overlap in both directions. i.e., a small fraction of G69-M1 peaks overlap with peaks from the other replicates (across) and a small fraction of peaks in other replicates overlap with G69-M1 peaks (down). Bar charts show overlap with DNase hypersensitivity sites and literature K4me3 sites (Robertson et al., 2008) . The fraction of peaks that are within 150 bp of ~73,000 standard DHS sites, ~110,000 total DHS sites, and of K4me3 sites in female liver from Robertson et al. One male sample was excluded due to low peak overlap with other replicates (lowest overlap 67% and lowest correlation 0.91) and low overlap with standard DHS (70%), all DHS (71%), and Robertson et al K4me1 peaks (71%).

Fraction of peaks in column sample that were found in row sample

K4me3 male	total peaks	G69_M2	G75_M4	G75_M5a	G75_M6a	All males
G69_M2	20883		66%	79%	80%	90%
G75_M4	15362	88%		92%	86%	95%
G75_M5a	14726	88%	78%		91%	98%
G75_M6a	14898	88%	76%	89%		97%
All males	16447	84%	67%	80%	81%	

correlation between reads in peaks

K4me3M	G69_M2	G75_M4	G75_M5	G75_M6
G69_M2		0.94	0.93	0.93
G75_M4	0.94		0.99	0.99
G75_M5	0.93	0.99		1.00
G75_M6	0.93	0.99	1.00	

Fraction of peaks in column sample that were found in row sample

K4me3 female	total peaks	G69_M3	G69_M4	G75_M8a	All females
G69_M3	21675		82%	71%	95%
G69_M4	21405	82%		69%	91%
G75_M8a	13343	96%	94%		98%
All females	19814	84%	81%	64%	

correlation between reads in peaks

K4me3F	G69_M3	G69_M4	G75_M8
G69_M3		0.97	0.83
G69_M4	0.97		0.81
G75_M8	0.83	0.81